J. Math. Anal. Appl. 537 (2024) 128287

Contents lists available at ScienceDirect

Journal of Mathematical Analysis and Applications

journal homepage: www.elsevier.com/locate/jmaa

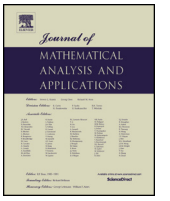

Regular Articles

Multi-breathers and higher-order rogue waves on the periodic background in a fourth-order integrable nonlinear Schrödinger equation

Yun-Chun Wei [a], Hai-Qiang Zhang [a,*], Wen-Xiu Ma [b,c,d,e]

[a] College of Science, University of Shanghai for Science and Technology, Shanghai 200093, China
[b] Department of Mathematics, Zhejiang Normal University, Jinhua 321004, Zhejiang, China
[c] Department of Mathematics, King Abdulaziz University, Jeddah 21589, Saudi Arabia
[d] Department of Mathematics and Statistics, University of South Florida, Tampa, FL 33620-5700, USA
[e] School of Mathematical and Statistical Sciences, North-West University, Mafikeng Campus, Private Bag X2046, Mmabatho 2735, South Africa

ARTICLE INFO

Article history:
Received 24 September 2023
Available online 7 March 2024
Submitted by G.M. Coclite

Keywords:
Darboux transformation
Elliptic functions
Breathers
Rogue waves
Fourth-order nonlinear Schrödinger equation

ABSTRACT

In this paper, we present a systematic formulation of multi-breathers and higher-order rogue wave solutions of a fourth-order nonlinear Schrödinger equation on the periodic background. First of all, we compute a complete family of elliptic solution of this higher-order equation, which can degenerate into two particular cases, i.e., the dnoidal and cnoidal solutions. By using the modified squared wavefunction approach, we solve the spectral problem on the elliptic function background. Then, we derive multi-breather solutions in terms of the theta functions, particular examples of which are the Kuznetsov-Ma breather and the Akhmediev breather. Furthermore, taking the limit of the breather solutions at branch points, we construct higher-order rogue wave solutions by employing a generalized Darboux transformation technique. On the periodic background, we present the first-order, second-order and second-second-order rogue waves. With aid of the theta functions, we explicitly characterize the resulting breathers and rogue waves, and demonstrate their dynamic behaviors by illustrative examples. Finally, we discuss how the parameter of the higher-order effects affects the breathers and rogue waves.

1. Introduction

It is well known that integrable nonlinear evolution equations play an important role in nonlinear science, and their localized solutions, solitons, breathers and rogue waves, have attracted great attention [1,16,29,41,54]. As a kind of nonlinear waves, rogue waves usually appear in the oceans with a significantly larger amplitude than the surrounding waves, and they often come from nowhere and disappear without any

* Corresponding author.
E-mail address: hqzhang@usst.edu.cn (H.-Q. Zhang).

https://doi.org/10.1016/j.jmaa.2024.128287
0022-247X/

trace [3,38]. The emergence of rogue waves is thought to be associated with the modulation instability of the plane waves or periodic waves [6]. On mathematical aspect, as the lowest-order rational solution to the nonlinear Schrödinger (NLS) equation, the Peregrine soliton, first proposed by Peregrine in 1983 [55], plays an important role in understanding the mechanics of the rogue wave phenomena. It is a doubly localized wave packet with a peaked hump and two side holes. Moreover, the maximum amplitude of the wave packet reaches three times the amplitude of the background plane wave. The Peregrine soliton solution can also be derived by taking the larger-period limitation of Kuznetsov-Ma breathers (KMBs) [39,45] or Akhmediev breathers (ABs) [2]. In recent years, many efforts have been made to realize the higher-order rogue waves of the NLS equation [14,34,52]. In addition, rogue waves have been experimentally observed in many physical settings including nonlinear optics [48,60,66], Bose-Einstein condensates [8,59] and plasma physics [27,62]. These important studies show that rogue waves can indeed be excited from a finite continuous background wave. More and more numerical and experimental evidence have shown that there are many new nonlinear physical phenomena that are related to rogue waves and breathers. For example, the excitation for rogue waves has been proposed [44] in media with electromagnetically induced transparency [24,49].

In the past decades, the field of rogue waves has rapidly grown. Recently, there has been considerable attention paid to rogue waves on a periodic background [7,10,23,63]. It has been shown that rogue waves can also arise due to the modulational instability of the periodic waves. Rogue waves on the periodic background have many rich physical properties and dynamic behaviors [22,35,51]. In Ref. [10] such exact solutions to the NLS equation were constructed first by combining the method of nonlinearization of spectral problem with the Darboux transformation (DT) method. Further, breathers and rogue waves for the NLS equation on the elliptic function background have also been presented by combining the algebro-geometric method and the squared wave function approach [23]. Recent studies reveal that rogue waves on the periodic function background are universal solutions of majority of integrable models [11,42,53,67,72]. In addition, it is worthwhile mentioning that rogue waves on the background of on stationary periodic waves have been experimentally observed in nonlinear optics and hydrodynamics [65]. Very recently, some achievements have been made on the solutions of breathers and rogue waves on the periodic background for the integrable equations associated with higher-order spectral problems, such as the vector Geng-Li model [28] and the Yajima-Oikawa long-wave-short-wave equation [43].

The NLS equation has limitations related to realistic problems, as there are also other significant physical effects that need to be considered. For instance, the ultrashort pulse propagation in optical fibers, aside from the group-velocity dispersion and Kerr nonlinearity, higher-order effects need to be taken into account, like the higher-order dispersion, self-steepening and self-frequency shift. Therefore, many extended NLS equation have been proposed by adding high-order terms with more free parameters. Recently, Ankiewicz et al. have proposed an extension of the NLS equation to the infinite NLS hierarchy with an arbitrary number of higher-order terms and free real coefficients [5,36]. This extension can be used to model various physical problems of nonlinear wave evolutions with a large degree of flexibility. Particularly, under different reduced coefficients, besides the NLS equation, this extension also includes many important integrable nonlinear equations such as the Hirota equation [30], the Lakshmanan-Porsezian-Daniel (LPD) equation [40] and the quintic NLS equation [17]. In the past few years, a large number of exact rogue wave or breather solutions of many equations in NLS hierarchy have been investigated on various backgrounds. Moreover, recent studies have shown that the higher-order effects in NLS hierarchy affect spatiotemporal patterns of rogue waves and cause the compression effects of the breathers [64,73]. For example, rogue waves for the Hirota equation on a uniform background [4] and on the dn/cn background [50] have been studied using different methods. Dynamical evolution behaviors of rogue waves and rational solitons for the quintic NLS equation have been detailed [68]. Meanwhile, in Ref. [18] researchers have found that a breather solution for the quintic NLS equation can be converted into a non-pulsating soliton solution.

In this paper, we study the following fourth-order NLS equation

$$\mathrm{i}q_t + \alpha\left(q_{xx} + 2|q|^2 q\right) + \beta\left(q_{xxxx} + 6\bar{q}q_x^2 + 4|q_x|^2 q + 8|q|^2 q_{xx} + 2q^2\bar{q}_{xx} + 6|q|^4 q\right) = 0, \tag{1}$$

where $q(x,t)$ is the slowly varying wave packet envelope, x, t respectively are the scaled spatial and time coordinate, the bar refers to the complex conjugate, the subscripts denote the partial derivatives, α and β are real parameters and stand for the strength of higher-order linear and nonlinear effects. Eq. (1) is also called the LPD equation, which was originally derived as a model for the nonlinear spin excitations in the one-dimensional isotropic biquadratic Heisenberg ferromagnetic spin [21,57]. It also arises in alpha helical proteins modeling the dynamics of higher-order molecular excitations associated with the energy transport [20]. In nonlinear optics, besides the group-velocity dispersion and Kerr nonlinearity, Eq. (1) can model the propagation of ultrashort optical pulses with the fourth-order dispersion, cubic-quintic nonlinearity, self-steepening and self-frequency shift [56]. Therefore, in contrast with the standard NLS equation, with the higher-order dispersions and nonlinearity effects, Eq. (1) can be applied to describe more complicated and real circumstance [46]. In the past decades, Eq. (1) has been investigated from different points of view, and its large classes of exact solutions have been studied extensively like the solitons, breathers and rogue waves [19,64,73].

In Ref. [71], we have obtained the first-order rogue wave solutions on the dn- and cn-elliptic function backgrounds. However, this algebraic method maybe is not very straightforward in use for generating multi-breather and high-order rogue wave solutions on the periodic background because it just only relies on the one- and two-fold potential transformations in the DT method. Therefore, in the present paper, we will give a systematic construction of multi-breather and higher-order rogue wave solutions for Eq. (1) on the elliptic function background, which can recover some previously published solutions. Since Eq. (1) is the third member in the NLS hierarchy of equations, its solutions can be studied in the same way as treating the NLS equation. However, it is a nontrivial work to construct multi-breather and higher-order rogue wave solutions on the background of elliptic functions because of the complexity of the time part in the Lax spectrum problem.

The method of the present study in solving the Lax spectrum problem is the modified squared wave (MSW) function approach [31–33], which is the so-called simple modification of the known finite-band integration method [25,26,70]. This method is based on the re-parametrization of the solution with the use of algebraic resolvent of the polynomial defining the solution in the finite-band integration method. The periodic solutions of nonlinear integrable equations can be constructed explicitly by introducing the Riemann surface of the hyperelliptic curve. It has been developed and applied to the investigation of the periodic solutions for many soliton equations [12,13,31–33,61] such as the NLS equation, the derivative NLS equation and the Heisenberg model.

In this paper, by use of the MSW function approach, we first solve the spectral problem of Eq. (1) corresponding to the Jacobi elliptic function seed solution. Then, with aid of the DT, we give the expression of multi-breather solution in terms of the determinant of theta functions based on the algebro-geometric method. Using the Taylor expansion technology and taking the special limit of the breather solutions at branch points, we derive higher-order rogue wave solutions by employing generalized DT. Based on obtained solutions, we analyze the dynamic behaviors of the breathers and rogue waves on the periodic background. We illustrate these results by discussing several examples. Finally, we discuss how the parameter of the higher-order effects affects the breathers and rogue waves.

The rest of this paper is arranged as the follows. In Section 2, we present the Lax pair, the multi-fold DT of Eq. (1) and the explicit formulas of the associated potential transformation. In Section 3, we derive the Jacobi elliptic function solutions of Eq. (1) and solve the Lax pair corresponding to the Jacobi elliptic function seed solution. In Section 4, we express these solutions in terms of the theta functions, and construct the multi-breather solution on the periodic background. In Section 5, by taking the special limit

of the breather solutions at branch points, we present higher-order rogue wave solutions. Furthermore, we analyze the dynamic behaviors of these solutions. In Section 6, by taking the KMB and the first-order rogue wave on the dn-periodic wave background as two illustrative examples, we discuss how the parameter of the higher-order effects affects the breathers and rogue waves. Section 7 is devoted to the conclusions.

2. Lax pair and Darboux transformation

To begin with, we write the Lax pair of Eq. (1) in the form [58]

$$\Psi_x = \mathbf{U}\Psi, \quad \Psi_t = \mathbf{V}\Psi, \tag{2}$$

with

$$\Psi = \begin{pmatrix} \psi_1(x,t;\lambda) & \psi_2(x,t;\lambda) \\ \phi_1(x,t;\lambda) & \phi_2(x,t;\lambda) \end{pmatrix}, \quad \mathbf{U} = \begin{pmatrix} F & G \\ H & -F \end{pmatrix}, \quad \mathbf{V} = \begin{pmatrix} A & B \\ C & -A \end{pmatrix},$$

and

$$\begin{aligned} &F = -\mathrm{i}\lambda, \quad G = \mathrm{i}q, \quad H = \mathrm{i}\bar{q}, \\ &A = -\mathrm{i}\alpha\left(2\lambda^2 - q\bar{q}\right) + \mathrm{i}\beta\left(\bar{q}(q_{xx} - 2\mathrm{i}\lambda q_x) - q_x\bar{q}_x + q(-4\lambda^2\bar{q} + 2\mathrm{i}\lambda\bar{q}_x + \bar{q}_{xx}) + 3q^2\bar{q}^2 + 8\lambda^4\right), \\ &B = \alpha\left(2\mathrm{i}\lambda q - q_x\right) + \beta\left(q(-6q_x\bar{q} - 8\mathrm{i}\lambda^3) + 4\mathrm{i}\lambda q^2\bar{q} + 4\lambda^2 q_x + 2\mathrm{i}\lambda q_{xx} - q_{xxx}\right), \\ &C = \alpha\left(\bar{q}_x + 2\mathrm{i}\lambda\bar{q}\right) + \beta\left(\bar{q}(-8\mathrm{i}\lambda^3 + 6q\bar{q}_x) - 4\lambda^2\bar{q}_x + 4\mathrm{i}\lambda q\bar{q}^2 + 2\mathrm{i}\lambda\bar{q}_{xx} + \bar{q}_{xxx}\right), \end{aligned}$$

where $(\psi_j, \phi_j)^T$ ($j = 1, 2$, the superscript T denotes the matrix transpose) are two vector solutions for the above linear eigenvalue problem, and λ is the spectral parameter. The compatibility condition $\Psi_{xt} = \Psi_{tx}$ or the zero curvature equation $\mathbf{U}_t - \mathbf{V}_x + [\mathbf{U}, \mathbf{V}] = 0$ is equivalent to Eq. (1).

It is well known that the DT method plays an important role in constructing explicit solutions of nonlinear integrable equations [47]. Suppose that $\Psi_i = (\psi_i, \phi_i)^T$ ($i = 1, 2, \ldots, n$) are a set of n linearly-independent solutions of the Lax pair (2) with $\lambda = \lambda_i$. Then, the n-fold DT of Eq. (1) can be constructed by:

$$\Psi[n] = \mathbf{T}[n]\Psi, \quad \mathbf{T}[n] = \mathbf{I} - \mathbf{X}_n\mathbf{M}_n^{-1}\mathbf{D}_n^{-1}\mathbf{X}_n^{\dagger}, \quad q[n] = q - 2\mathbf{X}_{n,1}{\mathbf{M}_{\mathbf{n}}}^{-1}\mathbf{X}_{n,2}^{\dagger}, \tag{3}$$

with

$$\mathbf{M}_n = \left(\frac{\Psi_i^{\dagger}\Psi_j}{\lambda_j - \lambda_i}\right)_{1\le i,j\le n}, \quad \mathbf{X}_n = [\Psi_1, \Psi_2, \ldots, \Psi_n], \quad \mathbf{D}_n = \mathrm{diag}(\lambda - \lambda_1, \lambda - \lambda_2, \ldots, \lambda - \lambda_n),$$

in which $\mathbf{X}_{n,k}$ ($k = 1, 2$) is the kth row of $\mathbf{X}_n$, $\mathbf{I}$ is the 2×2 identity matrix and the superscript $\dagger$ stands for the conjugate transpose. Moreover, based on the work in Refs. [23,29], we know that the above DT can be further generalized by a special limit, which is useful in constructing the higher-order soliton solutions. In this way, by expanding the Ψ_i at points $\lambda = \lambda_i$: $\Psi_i = \sum_{j=0}^{n_i-1} \Psi_i^{[j]}(\lambda - \lambda_i)^{[j]}$, so that the generalized DT can be formulated as follows: [23]

$$\mathbf{T}\left[m_1, m_2, \ldots, m_n\right] = \mathbf{I} - \mathbf{X}\mathbf{M}^{-1}\mathbf{D}^{-1}\mathbf{X}^{\dagger}, \quad q\left[m_1, m_2, \ldots, m_n\right] = q - 2\mathbf{X}_1\mathbf{M}^{-1}\mathbf{X}_2^{\dagger}, \tag{4}$$

with

$$\mathbf{X}=[X_1,X_2,\ldots,X_n],\quad \mathbf{M}=\mathbf{YSY}^{\dagger},$$
$$\mathbf{Y}=\begin{bmatrix} Y_1 & 0 & \cdots & 0\\ 0 & Y_2 & \cdots & 0\\ \vdots & \vdots & \ddots & \vdots\\ 0 & 0 & \cdots & Y_n\end{bmatrix},\quad \mathbf{D}=\begin{bmatrix} D_1 & 0 & \cdots & 0\\ 0 & D_2 & \cdots & 0\\ \vdots & \vdots & \ddots & \vdots\\ 0 & 0 & \cdots & D_n\end{bmatrix},\quad \mathbf{S}=\begin{bmatrix} S_{1,1} & S_{1,2} & \cdots & S_{1,n}\\ S_{2,1} & S_{2,2} & \cdots & S_{2,n}\\ \vdots & \vdots & \ddots & \vdots\\ S_{n,1} & S_{n,2} & \cdots & S_{n,n}\end{bmatrix},$$

and

$$X_a=\left[\Psi_a^{[0]},\Psi_a^{[1]},\ldots,\Psi_a^{[m_a-1]}\right],\quad S_{a,b}=\left(\frac{(-1)^{l+1}}{\left(\lambda_b-\bar{\lambda}_a\right)^{k+l-1}}\binom{k+l-2}{k-1}\right)_{1\le k\le m_a,1\le l\le m_b},$$
$$Y_a=\begin{bmatrix} \Psi_a^{[0]\dagger} & 0 & \cdots & 0\\ \Psi_a^{[1]\dagger} & \Psi_a^{[0]\dagger} & \cdots & 0\\ \vdots & \vdots & \ddots & \vdots\\ \Psi_a^{[m_a-1]\dagger} & \Psi_a^{[m_a-1]\dagger} & \cdots & \Psi_a^{[0]\dagger}\end{bmatrix},\quad D_a=\begin{bmatrix} \frac{1}{(\lambda-\bar{\lambda}_a)} & 0 & \cdots & 0\\ \frac{1}{(\lambda-\bar{\lambda}_a)^2} & \frac{1}{(\lambda-\bar{\lambda}_a)} & \cdots & 0\\ \vdots & \vdots & \ddots & \vdots\\ \frac{1}{(\lambda-\bar{\lambda}_a)^{m_a}} & \frac{1}{(\lambda-\bar{\lambda}_a)^{m_a-1}} & \cdots & \frac{1}{(\lambda-\bar{\lambda}_a)}\end{bmatrix}.$$

3. Jacobi elliptic function solutions and the solutions of Lax pair

In this section, we would like to exploit Jacobi elliptic function solutions of Eq. (1) and derive the corresponding solutions of the Lax pair (2) by the MSW function approach. We look for a wave solution to Eq. (1) of the following form

$$q(x,t)=\sqrt{u(x,t)}\exp(\mathrm{i}at),\tag{5}$$

where $u(x,t)$ is a positive real function to be determined and a is a real constant. First, we set two eigenfunctions of the Lax pair (2): $\Psi_1=(\psi_1,\phi_1)^{\mathrm{T}}$ and $\Psi_2=(\psi_2,\phi_2)^{\mathrm{T}}$, which are used to build a squared wave function via

$$f=-\frac{\mathrm{i}}{2}\left(\psi_1\phi_2+\psi_2\phi_1\right),\quad g=\psi_1\psi_2,\quad h=-\phi_1\phi_2.\tag{6}$$

In combination with the definition of f,g and h in Eqs. (6) and using the Lax pair (2), we get

$$f_x=-\mathrm{i}Hg+\mathrm{i}Gh,\quad g_x=2\mathrm{i}Gf+2Fg,\quad h_x=-2\mathrm{i}Hf-2Fh,\tag{7}$$
$$f_t=-\mathrm{i}Cg+\mathrm{i}Bh,\quad g_t=2\mathrm{i}Bf+2Ag,\quad h_t=-2\mathrm{i}Cf-2Ah.\tag{8}$$

Based on the Eqs. (7) and (8), one can find that $y^2(\lambda)\equiv f^2-gh$ is independent of x and t and is only the function of λ. Next we want to derive quasi-periodic solutions of Lax pair (2) in the presence of periodic background. It is known that periodic and quasi-periodic solutions of integrable evolution equations are associated with Riemann surfaces in the algebro-geometric theory [7]. In our situation, we consider such a surface determined by the following polynomial

$$y^2=f^2-gh=\prod_{i=1}^{4}(\lambda-\lambda_i)=\lambda^4-s_1\lambda^3+s_2\lambda^2-s_3\lambda+s_4,\tag{9}$$

where λ_i are zeros of the polynomial which parameterize the genus-1 solution. Eqs. (7) and (8) have a solution in the polynomial forms of f,g and h:

$$f = \lambda^2 - f_1(x,t)\lambda + f_2(x,t), \quad g = \mathrm{i}q(x,t)(\lambda - \mu(x,t)), \quad h = \mathrm{i}\bar{q}(x,t)\left(\lambda - \bar{\mu}(x,t)\right). \tag{10}$$

By comparing the coefficients of λ^k on both sides of Eq. (9), we obtain

$$f_1(x,t) = \frac{1}{2}s_1, \quad f_2(x,t) = \frac{1}{2}(p_1 - u(x,t)), \tag{11}$$

$$\mu(x,t) + \bar{\mu}(x,t) = \frac{1}{2}s_1 - \frac{1}{u(x,t)}p_2, \quad \mu(x,t)\bar{\mu}(x,t) = -\frac{1}{4u(x,t)}\left(u^2(x,t) - 2p_1u(x,t) + p_1^2 - 4s_4\right), \tag{12}$$

where

$$p_1 = s_2 - \frac{1}{4}s_1^2, \quad p_2 = \frac{1}{2}s_1\left(s_2 - \frac{1}{4}s_1^2\right) - s_3. \tag{13}$$

From the above expressions (12), we can derive the exact expressions of μ and $\bar{\mu}$

$$\mu,\, \bar{\mu} = \frac{1}{4}s_1 - \frac{p_2 \pm \mathrm{i}\sqrt{-R(u)}}{2u(x,t)}, \tag{14}$$

where

$$R(u) = u^3(x,t) + (s_1^2/4 - 2p_1)u^2(x,t) + (p_1^2 - s_1p_2 - 4s_4)u(x,t) + p_2^2. \tag{15}$$

From the first equation in Eqs. (11), the function $f_1(x,t)$ is a constant determining the phase velocity of the background periodic wave. For simplicity, we consider the case of $f_1 = 0$. The case of $f_1 \neq 0$ can be similarly treated as the case of $f_1 = 0$. In order to satisfy $f_1 = 0$ and $u(x,t) > 0$, the zeros λ_i need to be formed by two pairs of specific complex numbers and their complex conjugates

$$\lambda_1 = b + \mathrm{i}c, \quad \lambda_2 = -b + \mathrm{i}d, \quad \lambda_3 = b - \mathrm{i}c, \quad \lambda_4 = -b - \mathrm{i}d, \tag{16}$$

where b, c and d are positive real constants. In addition, when the polynomial (15) admits three zeros u_j $(j = 1, 2, 3)$, then through a direct calculation, we can derive the relations between the roots and the coefficients:

$$u_1 = -\frac{1}{4}(\lambda_1 + \lambda_3 - \lambda_2 - \lambda_4)^2, \quad u_2 = -\frac{1}{4}(\lambda_1 + \lambda_4 - \lambda_2 - \lambda_3)^2, \quad u_3 = -\frac{1}{4}(\lambda_1 + \lambda_2 - \lambda_3 - \lambda_4)^2, \tag{17}$$

and

$$s_1 = 0, \quad s_2 = \frac{1}{2}\left(u_1 + u_2 + u_3\right), \quad s_3 = \sqrt{-u_1u_2u_3}, \quad s_4 = \frac{1}{16}\left(u_1^2 - 2\left(u_2 + u_3\right)u_1 + \left(u_2 - u_3\right)^2\right). \tag{18}$$

Meanwhile, by inserting Eqs. (16) into Eqs. (17), we obtain $u_1 = -4b^2$, $u_2 = (c-d)^2$ and $u_3 = (c+d)^2$. Using Eqs. (6)-(8) and taking $\lambda = \mu$, one can obtain

$$\mu_x = -2\mathrm{i}\sqrt{f(\mu)} = -2\mathrm{i}y(\mu), \quad \mu_t = -4\beta s_3\mu_x. \tag{19}$$

Based on Eqs. (7) and (8), we further derive the expression of u with respect to x and t

$$u_x = 2\sqrt{-R(u)}, \quad u_t = -4\beta s_3u_x. \tag{20}$$

Since $R(u)$ is a cubic polynomial and $u_1 \leq 0 \leq u_2 < u_3$, the explicit expression of u is readily obtained in terms of the Jacobi elliptic function

$$u\left(x-4\beta s_3 t\right)=u_3+\left(u_2-u_3\right)\mathrm{sn}^2\left(\sqrt{u_3-u_1}\left(x-4\beta s_3 t\right);m\right), \tag{21}$$

where $m=\sqrt{\frac{u_3-u_2}{u_3-u_1}}$. Moreover, from Eqs. (7), (8) and (10), we find that

$$q_x=2\mathrm{i}\mu q=\mathrm{i}\frac{s_3}{u}q+(\frac{1}{2}\ln u)_x q,\quad q_t=2\mathrm{i}\left(\alpha s_2+\beta(3s_2^2-4s_4)\right)q-4\beta s_3 q_x. \tag{22}$$

Based on the results of Eqs. (20) and Eqs. (22), we deduce that

$$q(x,t)=\sqrt{u_3+\left(u_2-u_3\right)\mathrm{sn}^2\left(\sqrt{u_3-u_1}x;m\right)}\exp\left(2\mathrm{i}\left[\alpha s_2+\beta(3s_2^2-4s_4)\right]t\right), \tag{23}$$

where we have set $s_3=0$ for convenience. Therefore, under this condition $s_3=\sqrt{-u_1u_2u_3}=0$, the solution (23) can reduce to the following two types of Jacobi elliptic function solutions

(i) For $u_1=0$ (i.e., $b=0$)

$$q(x,t)=k\,\mathrm{dn}\left(kx;m\right)\exp(\mathrm{i}at), \tag{24}$$

where $k=c+d$, $m=\sqrt{\frac{4cd}{(c+d)^2}}$ and $a=2\left[\alpha\left(c^2+d^2\right)+\beta\left(3c^4+2c^2d^2+3d^4\right)\right]$.

(ii) For $u_2=0$ (i.e., $c=d$)

$$q(x,t)=km\,\mathrm{cn}(kx;m)\exp(\mathrm{i}at), \tag{25}$$

where $k=2\sqrt{b^2+d^2}$, $m=\sqrt{\frac{d^2}{b^2+d^2}}$ and $a=4\left[\alpha\left(d^2-b^2\right)+4\beta\left(b^4-4b^2d^2+d^4\right)\right]$.

Next, we proceed to construct the solutions of the Lax pair (2) on the background of the periodic solutions (24) and (25) using the MSW approach. By defining $w_j\equiv\frac{\phi_j}{\psi_j}$ $(j=1,2)$ and using Eqs. (6), we have

$$f(x,t;\lambda)=\frac{\mathrm{i}}{2}\left(\frac{h(x,t;\lambda)}{w_j(x,t;\lambda)}-g(x,t;\lambda)w_j(x,t;\lambda)\right),$$

which implies that

$$\begin{aligned}w_1(x,t;\lambda)&=\mathrm{i}\left(\frac{f(x,t;\lambda)+y}{g(x,t;\lambda)}\right)=\mathrm{i}\left(\frac{h(x,t;\lambda)}{f(x,t;\lambda)-y}\right),\\ w_2(x,t;\lambda)&=\mathrm{i}\left(\frac{f(x,t;\lambda)-y}{g(x,t;\lambda)}\right)=\mathrm{i}\left(\frac{h(x,t;\lambda)}{f(x,t;\lambda)+y}\right).\end{aligned} \tag{26}$$

Then, from the Lax pair (2), the functions ψ_1 and ϕ_1 in Ψ_1 can be derived as:

$$(\ln\psi_1)_x=F+Gw_1,\quad (\ln\phi_1)_x=H\frac{1}{w_1}-F. \tag{27}$$

$$(\ln\psi_1)_t=A+Bw_1,\quad (\ln\phi_1)_t=C\frac{1}{w_1}-A. \tag{28}$$

Inserting Eqs. (10) into Eqs. (27) and combining w_1 in Eqs. (26), we have

$$(\ln\psi_1)_x = -\mathrm{i}\lambda - \frac{h(x,t;\lambda)}{f(x,t;\lambda)-y}q(x,t) = \mathrm{i}\lambda + \mathrm{i}\frac{C_1}{u(x)-2\gamma_1} + \frac{1}{2}\ln\left(u(x)-2\gamma_1\right)_x,$$
$$(\ln\phi_1)_x = \mathrm{i}\lambda + \frac{g(x,t;\lambda)}{f(x,t;\lambda)+y}\bar{q}(x,t) = -\mathrm{i}\lambda - \mathrm{i}\frac{C_2}{u(x)-2\gamma_2} + \frac{1}{2}\ln\left(u(x)-2\gamma_2\right)_x,$$

where $C_j = 4\lambda\gamma_j$ and $\gamma_j = \lambda^2 + s_2/2 \mp y$ ($\mp$ symbol: the upper sign is for $j=1$ and the lower sign is for $j=2$). Integrating with respect to x once for the above equations gives

$$\ln\psi_1 = \mathrm{i}\lambda x + \mathrm{i}\int_0^x \frac{C_1\,\mathrm{d}s}{u(s)-2\gamma_1} + \frac{1}{2}\ln\left(u(x)-2\gamma_1\right) + D_1(t), \tag{29}$$

$$\ln\phi_1 = -\mathrm{i}\lambda x - \mathrm{i}\int_0^x \frac{C_2\,\mathrm{d}s}{u(s)-2\gamma_2} + \frac{1}{2}\ln\left(u(x)-2\gamma_2\right) + D_2(t). \tag{30}$$

With the aid of Eqs. (19) and Eqs. (22), we insert the high-order derivative of μ and q with respect to x into Eqs. (28), we arrive at

$$(\ln\psi_1)_t = \mathrm{i}\alpha\left(2y+s_2\right) + \mathrm{i}\beta(P_1 y + P_0), \quad (\ln\phi_1)_t = \mathrm{i}\alpha\left(2y-s_2\right) + \mathrm{i}\beta(P_1 y - P_0), \tag{31}$$

where

$$P_1 = 4s_2 - 8\lambda^2 - \frac{4u(x)\left[\bar{\mu}(x)+\mu(x)\right]}{\lambda-\mu(x)},$$
$$P_0 = -\left(u(x)\left[4\mu(x)\bar{\mu}(x)+u(x)\right] - 2s_2u(x) - 2s_2^2\right) + \frac{2u(x)\left[\bar{\mu}(x)+\mu(x)\right]\left(-2\lambda\mu(x)-s_2+u(x)\right)}{\lambda-\mu(x)}.$$

By use of $\mu\bar{\mu} = -\frac{1}{4u}\left(u^2 - 2s_2u + s_2^2 - 4s_4\right)$ and $\bar{\mu}+\mu = 0$ in Eqs. (12), the P_1 and P_0 can be simplified as

$$P_1 = 4s_2 - 8\lambda^2, \quad P_0 = 3s_2^2 - 4s_4. \tag{32}$$

Furthermore, based on Eqs. (29)-(32), the ψ_1 and ϕ_1 can be given by

$$\psi_1(x,t;\lambda) = B_1\sqrt{u(x)-2\gamma_1}\exp\left(\theta_1\right), \quad \theta_1 = \mathrm{i}\int_0^x \frac{C_1\,\mathrm{d}s}{u(s)-2\gamma_1} + \mathrm{i}\lambda x + \mathrm{i}D_1 t, \tag{33}$$

$$\phi_1(x,t;\lambda) = B_2\sqrt{u(x)-2\gamma_2}\exp\left(\theta_2\right), \quad \theta_2 = -\mathrm{i}\int_0^x \frac{C_2\,\mathrm{d}s}{u(s)-2\gamma_2} - \mathrm{i}\lambda x + \mathrm{i}D_2 t, \tag{34}$$

where $D_j = \alpha\left(2y \pm s_2\right) + \beta\left[y\left(4s_2 - 8\lambda^2\right) \pm \left(3s_2^2 - 4s_4\right)\right]$, and the B_j $(j=1,2)$ stand for two complex constants to be determined. According to the definition: $w_1 \equiv \frac{\phi_1}{\psi_1}$, one can derive that

$$w_1(0,0;\lambda) = \mathrm{i}\sqrt{\frac{f(0,0;\lambda)+y}{f(0,0;\lambda)-y}}\sqrt{\frac{h(0,0;\lambda)}{g(0,0;\lambda)}} = \mathrm{i}\sqrt{\frac{u(0)-2\gamma_2}{u(0)-2\gamma_1}} \equiv \frac{B_2}{B_1}\sqrt{\frac{u(0)-2\gamma_2}{u(0)-2\gamma_1}}. \tag{35}$$

For simplicity, we consider $B_1 = 1$ and $B_2 = \mathrm{i}$.

By using a similar procedure as in ϕ_1 and ψ_1, we can also obtain the other vector solution of the Lax pair (2) as follows:

$$\psi_2(x,t;\lambda) = \sqrt{u(x)-2\gamma_2}\exp\left(-\theta_2\right), \quad \phi_2(x,t;\lambda) = \mathrm{i}\sqrt{u(x)-2\gamma_1}\exp\left(-\theta_1\right). \tag{36}$$

Therefore, one fundamental solution for the Lax pair (2) with q as the elliptic function (23) can be represented as:

$$\Psi(x,t;\lambda)=\begin{bmatrix}\sqrt{u(x)-2\gamma_1}\mathrm{e}^{\theta_1} & \sqrt{u(x)-2\gamma_2}\mathrm{e}^{-\theta_2}\\ \mathrm{i}\sqrt{u(x)-2\gamma_2}\mathrm{e}^{\theta_2} & \mathrm{i}\sqrt{u(x)-2\gamma_1}\mathrm{e}^{-\theta_1}\end{bmatrix}. \tag{37}$$

4. Theta function representation for solutions and multi-breather solution

To begin with, we will use theta functions to express the solutions q, ψ_j and ϕ_j $(j=1,2)$. Based on Eqs. (19), we know that the spectra curve (9) as genus-1 Riemann surface can be parameterized by the uniformization variable z [7,63]

$$y(z)=\frac{k}{2}\frac{\mathrm{d}}{\mathrm{d}z}\mu\left(\frac{\mathrm{i}(z-l)}{k}\right),\quad \lambda(z)=\mu\left(\frac{\mathrm{i}(z-l)}{k}\right), \tag{38}$$

with $k=\sqrt{u_3-u_1}$ and $l\in\left[\frac{-K'}{2},\frac{K'}{2}\right]$, where $K'=K(1-m)$ and $K(m)$ is the complete elliptic integral of the first kind. Furthermore, in order to deduce the solutions of the Lax pair (2) with a uniform expression for different l, we introduce the parameterization:

$$u_1=-k^2\mathrm{dn}^2(a_0;m),\quad u_2=-m^2k^2\mathrm{cn}^2(a_0;m),\quad u_3=m^2k^2\mathrm{sn}^2(a_0;m),\ \ a_0=K+2\mathrm{i}l. \tag{39}$$

Combining Eqs. (18) and Eq. (21), we have $u(x)=k^2\left(\mathrm{dn}^2(kx;m)-\mathrm{dn}^2(a_0;m)\right)$ and $s_2=\frac{k^2}{2}(2-m^2-3\mathrm{dn}^2(a_0;m))$. Obviously, when $l_d=\frac{K'}{2}$ and $l_c=0$, $u(x)$ can reduce to the Jacobi elliptic dn and cn functions, respectively. Moreover, with the aid of the associated transformation relationship (see appendix B of Ref. [63]), we can derive directly the solutions q in terms of the theta functions:

$$q_d(x,t)=k\frac{\vartheta_4\vartheta_3\left(\frac{kx}{2K}\right)}{\vartheta_3\vartheta_4\left(\frac{kx}{2K}\right)}\exp(\mathrm{i}at),\quad q_c(x,t)=k\frac{\vartheta_2\vartheta_4\vartheta_2\left(\frac{kx}{2K}\right)}{\vartheta_3^2\vartheta_4\left(\frac{kx}{2K}\right)}\exp(\mathrm{i}at). \tag{40}$$

To continue, according to the definition of $\mu:=-\frac{\mathrm{i}}{4}\ln(u)_x$, taking $\lambda=\mu$ in Eqs. (38), we can obtain the corresponding $\lambda(z)$ of Eqs. (40) as follows:

$$\lambda_d(z)=\frac{\mathrm{i}}{2}km^2\,\mathrm{sn}(\mathrm{i}(z-l))\,\mathrm{cd}(\mathrm{i}(z-l)),\quad \lambda_c(z)=\frac{\mathrm{i}}{2}k\mathrm{dn}(\mathrm{i}(z-l))\,\mathrm{sc}(\mathrm{i}(z-l)).$$

Hereafter, for simplicity, we omit the modulus parameter m. Using the addition formulas of the Jacobi elliptic functions (see 122.18 of Ref. [9]), the above expressions can be rewritten as one formula for different l (i.e., l_d or l_c):

$$\lambda(z)=\frac{\mathrm{i}}{2}k\left[\mathrm{dn}(2\mathrm{i}l)\mathrm{dn}(\mathrm{i}(z-l))\,\mathrm{sc}(\mathrm{i}(z+l))-m\mathrm{cn}(2\mathrm{i}l)\mathrm{sd}(2\mathrm{i}l)\right]. \tag{41}$$

On account of Eqs. (38), we can write $y(z)$ in the form:

$$y_d(z)=\frac{1}{4}k^2m^2\left(\mathrm{sn}(\mathrm{i}(z-l))^2-\mathrm{cd}(\mathrm{i}(z-l))^2\right),\quad y_c(z)=\frac{1}{4}k^2\left(m^2\mathrm{sn}(\mathrm{i}(z-l))^2-\mathrm{dc}(\mathrm{i}(z-l))^2\right).$$

Furthermore, the above two equations can merge into one

$$y(z)=\frac{1}{4}k^2\left(\mathrm{dn}^2(a_2)-\mathrm{dn}^2(a_1)\right), \tag{42}$$

where $a_1 = \mathrm{i}(z-l)$ and $a_2 = K + \mathrm{i}K' - \mathrm{i}(z+l)$. In order to simplify parametrization of the solutions, we consider a better formula of $\lambda^2(z)$ by the addition formula

$$\lambda^2(z) = \frac{1}{4}k^2\left(\mathrm{dn}^2(a_0) + \mathrm{dn}^2(a_1) + \mathrm{dn}^2(a_2) + m^2 - 2\right). \tag{43}$$

With these results, we obtain

$$\gamma_j = \lambda^2(z) + \frac{1}{2}s_2 \mp y(z) = \frac{1}{2}k^2\left(\mathrm{dn}^2(a_j) - \mathrm{dn}^2(a_0)\right), \qquad (j = 1, 2). \tag{44}$$

Meanwhile, we have $u(x) - 2\gamma_j = k^2\left(\mathrm{dn}^2(kx) - \mathrm{dn}^2(a_j)\right) = k^2m^2\left(\mathrm{sn}^2(a_j) - \mathrm{sn}^2(kx)\right)$. Based on Eqs. (9) and (38), we know that $2y\frac{\mathrm{dy}}{\mathrm{d}\lambda} = 4\lambda^3 + 2s_2\lambda$, and thus the C_j can be derived as

$$C_j = 4\lambda(z)\gamma_j = 2y(z)\left(\frac{\mathrm{d}y(z)}{\mathrm{d}\lambda(z)} \mp 2\lambda(z)\right) = k\frac{\mathrm{d}}{\mathrm{d}z}\left(y(z) \mp \lambda^2(z)\right) = \mathrm{i}k^3m^2\mathrm{sn}(a_j)\mathrm{cn}(a_j)\mathrm{dn}(a_j). \tag{45}$$

Next, we will present the elements of the solutions (37) in terms of theta functions. By utilizing the integration formula (see appendix B of Ref. [63]), one can derive

$$\int_0^x \frac{\mathrm{i}C_j}{u(s) - 2\gamma_j}\mathrm{d}s = \int_0^{kx} \frac{\mathrm{sn}(a_j)\,\mathrm{cn}(a_j)\mathrm{dn}(a_j)}{\mathrm{sn}^2(s) - \mathrm{sn}^2(a_j)}\mathrm{d}s = \frac{1}{2}\ln\frac{\vartheta_1\left(\frac{a_j - kx}{2K}\right)}{\vartheta_1\left(\frac{a_j + kx}{2K}\right)} + kZ(a_j)x. \tag{46}$$

Using the addition formula of theta functions (see 3.4 of Ref. [37]), we get

$$u(x) - 2\gamma_j = k^2\frac{\vartheta_2^2}{\vartheta_3^2}\left(\frac{\vartheta_1^2\left(\frac{a_j}{2K}\right)}{\vartheta_4^2\left(\frac{a_j}{2K}\right)} - \frac{\vartheta_1^2\left(\frac{kx}{2K}\right)}{\vartheta_4^2\left(\frac{kx}{2K}\right)}\right) = k^2\frac{\vartheta_2^2}{\vartheta_3^2}\frac{\vartheta_4^2\vartheta_1\left(\frac{a_j + kx}{2K}\right)\vartheta_1\left(\frac{a_j - kx}{2K}\right)}{\vartheta_4^2\left(\frac{a_j}{2K}\right)\vartheta_4^2\left(\frac{kx}{2K}\right)}. \tag{47}$$

Then, by inserting the above two equations into Eq. (37), we have

$$\psi_1(x,t;z) = \frac{k\vartheta_2\vartheta_4}{\vartheta_3\vartheta_4\left(\frac{kx}{2K}\right)}\frac{\vartheta_1\left(\frac{\mathrm{i}(z-l)-kx}{2K}\right)}{\vartheta_4\left(\frac{\mathrm{i}(z-l)}{2K}\right)}\mathrm{e}^{E_1x + \mathrm{i}D_1t}, \quad \phi_1(x,t;z) = \frac{\mathrm{i}k\vartheta_2\vartheta_4}{\vartheta_3\vartheta_4\left(\frac{kx}{2K}\right)}\frac{\vartheta_3\left(\frac{\mathrm{i}(z+l)-kx}{2K}\right)}{\vartheta_2\left(\frac{\mathrm{i}(z+l)}{2K}\right)}\mathrm{e}^{E_2x + \mathrm{i}D_2t},$$

and

$$\psi_2(x,t;z) = \frac{k\vartheta_2\vartheta_4}{\vartheta_3\vartheta_4\left(\frac{kx}{2K}\right)}\frac{\vartheta_3\left(\frac{\mathrm{i}(z+l)+kx}{2K}\right)}{\vartheta_2\left(\frac{\mathrm{i}(z+l)}{2K}\right)}\mathrm{e}^{-E_2x - \mathrm{i}D_2t}, \quad \phi_2(x,t;z) = \frac{\mathrm{i}k\vartheta_2\vartheta_4}{\vartheta_3\vartheta_4\left(\frac{kx}{2K}\right)}\frac{\vartheta_1\left(\frac{\mathrm{i}(z-l)+kx}{2K}\right)}{\vartheta_4\left(\frac{\mathrm{i}(z-l)}{2K}\right)}\mathrm{e}^{-E_1x - \mathrm{i}D_1t},$$

where $E_1 = kZ(\mathrm{i}(z-l)) + \mathrm{i}\lambda$ and $E_2 = -\frac{\mathrm{i}k\pi}{2K} - kZ(K + \mathrm{i}K' - \mathrm{i}(z+l)) - \mathrm{i}\lambda$. Using the addition formulas of the Zeta function (see 142 of Ref. [9]), we get

$$\begin{aligned}
Z_1 &= Z(K + \mathrm{i}K' - \mathrm{i}(z+l)) \\
&= Z(-\mathrm{i}(z-l)) + Z\left(K + \mathrm{i}K' - 2\mathrm{i}l\right) + m^2\,\mathrm{sn}(\mathrm{i}(z-l))\,\mathrm{sn}\left(K + \mathrm{i}K' - 2\mathrm{i}l\right)\mathrm{sn}\left(K + \mathrm{i}K' - \mathrm{i}(z+l)\right) \\
&= -Z(\mathrm{i}(z-l)) - Z(K + 2\mathrm{i}l) + \mathrm{cs}(K - 2\mathrm{i}l)\,\mathrm{dn}(K - 2\mathrm{i}l) - \frac{\mathrm{i}\pi}{2K} \\
&\quad + m^2\,\mathrm{sn}(\mathrm{i}(z-l))\,\mathrm{sn}\left(K + \mathrm{i}K' - 2\mathrm{i}l\right)\mathrm{sn}\left(K + \mathrm{i}K' - \mathrm{i}(z+l)\right).
\end{aligned}$$

For $l = l_d$ or $l = l_c$, we find that the Z_1 can be further simplified into

$$Z_1 = -Z(\mathrm{i}(z-l)) - Z(K+2\mathrm{i}l) - \frac{\mathrm{i}\pi}{2K} - \frac{2\mathrm{i}}{k}\lambda(z). \tag{48}$$

Hence, the E_2 can be rewritten in the form

$$E_2 = kZ(\mathrm{i}(z-l)) + kZ(K+2\mathrm{i}l) + \mathrm{i}\lambda(z) = E_1 + kZ(K+2\mathrm{i}l). \tag{49}$$

Therefore, one fundamental solution for the Lax pair (2) with q represented by Eq. (40) can be expressed in terms of theta functions

$$\begin{bmatrix} \psi_1(x,t;z) \\ \phi_1(x,t;z) \end{bmatrix} = \frac{k\vartheta_2\vartheta_4}{\vartheta_3\vartheta_4\left(\frac{kx}{2K}\right)} \mathrm{e}^{E_1 x + \mathrm{i}\left[\alpha(2y+s_2)+\beta(y(4s_2-8\lambda^2)+(3s_2^2-4s_4))\right]t} \begin{bmatrix} \frac{\vartheta_1\left(\frac{\mathrm{i}(z-l)-kx}{2K}\right)}{\vartheta_4\left(\frac{\mathrm{i}(z-l)}{2K}\right)} \\ \frac{\mathrm{i}\vartheta_3\left(\frac{\mathrm{i}(z+l)-kx}{2K}\right)}{\vartheta_2\left(\frac{\mathrm{i}(z+l)}{2K}\right)} \mathrm{e}^{kZ(K+2\mathrm{i}l)x - 2\mathrm{i}\left[\alpha s_2+\beta(3s_2^2-4s_4)\right]t} \end{bmatrix} \tag{50}$$

and

$$\begin{bmatrix} \psi_2(x,t;z) \\ \phi_2(x,t;z) \end{bmatrix} = \frac{k\vartheta_2\vartheta_4}{\vartheta_3\vartheta_4\left(\frac{kx}{2K}\right)} \mathrm{e}^{-E_1 x - \mathrm{i}\left[\alpha(2y+s_2)+\beta(y(4s_2-8\lambda^2)+(3s_2^2-4s_4))\right]t} \begin{bmatrix} \frac{\vartheta_3\left(\frac{\mathrm{i}(z+l)+kx}{2K}\right)}{\vartheta_2\left(\frac{\mathrm{i}(z+l)}{2K}\right)} \mathrm{e}^{-kZ(K+2\mathrm{i}l)x + 2\mathrm{i}\left[\alpha s_2+\beta(3s_2^2-4s_4)\right]t} \\ \frac{\mathrm{i}\vartheta_1\left(\frac{\mathrm{i}(z-l)+kx}{2K}\right)}{\vartheta_4\left(\frac{\mathrm{i}(z-l)}{2K}\right)} \end{bmatrix}. \tag{51}$$

In the following, we construct multi-breather solutions of Eq. (1) on the background of the Jacobi elliptic functions. In this way, we consider the linear combination of the two sets of solutions

$$\begin{aligned} \Psi(x,t;z_i) &= \begin{bmatrix} \psi_1(x,t;z_i) \\ \phi_1(x,t;z_i) \end{bmatrix} + \alpha_i \begin{bmatrix} \psi_2(x,t;z_i) \\ \phi_2(x,t;z_i) \end{bmatrix} \\ &= G(x)\left(\omega_2(x,t;z_i)\begin{bmatrix} d_{14}(-x;z_i) \\ \mathrm{i}d_{32}(-x;z_i)\omega_1(x,t) \end{bmatrix} + \alpha_i\omega_2^{-1}(x,t;z_i)\begin{bmatrix} d_{32}(x;z_i)\omega_1^{-1}(x,t) \\ \mathrm{i}d_{14}(x;z_i) \end{bmatrix}\right), \end{aligned} \tag{52}$$

in which α_i is a complex constant, and

$$\begin{aligned} &\omega_1(x,t) := \exp\left(kZ(K+2\mathrm{i}l)x - 2\mathrm{i}\left[\alpha s_2 + \beta(3s_2^2-4s_4)\right]t\right), \\ &\omega_2(x,t;z_i) := \exp\left(kZ(\mathrm{i}(z-l))x + \mathrm{i}\lambda x + \mathrm{i}\left[\alpha(2y+s_2)+\beta(y(4s_2-8\lambda^2)+(3s_2^2-4s_4))\right]t\right), \\ &G(x) := \frac{k\vartheta_2\vartheta_4}{\vartheta_3\vartheta_4\left(\frac{kx}{2K}\right)}, \quad d_{14}(x;z_i) := \frac{\vartheta_1\left(\frac{\mathrm{i}(z_i-l)+kx}{2K}\right)}{\vartheta_4\left(\frac{\mathrm{i}(z_i-l)}{2K}\right)}, \quad d_{32}(x;z_i) := \frac{\vartheta_3\left(\frac{\mathrm{i}(z_i+l)+kx}{2K}\right)}{\vartheta_2\left(\frac{\mathrm{i}(z_i+l)}{2K}\right)}. \end{aligned}$$

Then, the complex conjugate of the solution (52) can be given by:

$$\bar{\Psi}(x,t;z_j) = G(x)\left(-\bar{\omega}_2(x,t;z_j)\begin{bmatrix} d_{14}(x;\bar{z}_j) \\ \mathrm{i}d_{32}(x;\bar{z}_j)\omega_1^{-1}(x,t) \end{bmatrix} + \bar{\alpha}_j\bar{\omega}_2^{-1}(x,t;z_j)\begin{bmatrix} d_{32}(-x;\bar{z}_j)\omega_1(x,t) \\ \mathrm{i}d_{14}(-x;\bar{z}_j) \end{bmatrix}\right). \tag{53}$$

Consequently, the potential transformation in Eq. (3) can be rewritten in this form:

$$q_n(x,t) = q(x,t)^{1-n}\frac{\det(\mathbf{H})}{\det(\mathbf{M})}, \quad \mathbf{M} = \left(\frac{\Psi^\dagger(z_j)\Phi(z_i)}{2\left(\lambda(z_i)-\lambda(\bar{z}_j)\right)}\right)_{1\le i,j\le n}, \quad \mathbf{H} = q(x,t)\mathbf{M} - \Phi_1\Phi_2, \tag{54}$$

where $\Phi_1 = [\Psi_1(z_1), \Psi_1(z_2), \ldots, \Psi_1(z_n)]$, $\Phi_2 = [\Psi_2(z_1), \Psi_2(z_2), \ldots, \Psi_2(z_n)]^\dagger$. Then, according to the representation of the solution for the NLS equation [23], we would like to use Eq. (52) and Eq. (53) to represent the elements in Eq. (54)

$$\begin{aligned}\Psi^\dagger(z_j)\Psi(z_i) = G(x)^2\big(&\omega_2(x,t;z_i)\bar{\omega}_2(x,t;z_j)\left[d_{32}(x;\bar{z}_j)d_{32}(-x;z_i) - d_{14}(x;\bar{z}_j)d_{14}(-x;z_i)\right]\\ &+\alpha_i\omega_1^{-1}(x,t)\omega_2^{-1}(x,t;z_i)\bar{\omega}_2(x,t;z_j)\left[d_{14}(x;z_i)d_{32}(x;\bar{z}_j) - d_{14}(x;\bar{z}_j)d_{32}(x;z_i)\right]\\ &+\bar{\alpha}_j\omega_1(x,t)\omega_2(x,t;z_i)\bar{\omega}_2^{-1}(x,t;z_j)\left[d_{14}(-x;z_i)d_{32}(-x;\bar{z}_j) - d_{14}(-x;\bar{z}_j)d_{32}(-x;z_i)\right]\\ &+\alpha_i\bar{\alpha}_j\omega_2^{-1}(x,t;z_i)\bar{\omega}_2^{-1}(x,t;z_j)\left[d_{32}(x;z_i)d_{32}(-x;\bar{z}_j) - d_{14}(x;z_i)d_{14}(-x;\bar{z}_j)\right]\big).\end{aligned} \tag{55}$$

The terms in square brackets can be simplified based on the addition formula for the theta functions (see 3.5b and 3.8 of Ref. [37]),

$$\left[d_{32}(x;\bar{z}_j)d_{32}(-x;z_i) - d_{14}(x;\bar{z}_j)d_{14}(-x;z_i)\right] = \frac{\vartheta_3\left(\frac{2il}{2K}\right)\vartheta_4\left(\frac{kx}{2K}\right)\vartheta_3\left(\frac{\mathrm{i}(z_i+\bar{z}_j)}{2K}\right)\vartheta_4\left(\frac{\mathrm{i}(z_i-\bar{z}_j)-kx}{2K}\right)}{\vartheta_2\left(\frac{\mathrm{i}(z_i+l)}{2K}\right)\vartheta_2\left(\frac{\mathrm{i}(\bar{z}_j+l)}{2K}\right)\vartheta_4\left(\frac{\mathrm{i}(z_i-l)}{2K}\right)\vartheta_4\left(\frac{\mathrm{i}(\bar{z}_j-l)}{2K}\right)},$$

$$\left[d_{14}(x;z_i)d_{32}(x;\bar{z}_j) - d_{14}(x;\bar{z}_j)d_{32}(x;z_i)\right] = \frac{\vartheta_3\left(\frac{2il}{2K}\right)\vartheta_4\left(\frac{kx}{2K}\right)\vartheta_1\left(\frac{\mathrm{i}(z_i-\bar{z}_j)}{2K}\right)\vartheta_2\left(\frac{\mathrm{i}(z_i+\bar{z}_j)+kx}{2K}\right)}{\vartheta_2\left(\frac{\mathrm{i}(z_i+l)}{2K}\right)\vartheta_2\left(\frac{\mathrm{i}(\bar{z}_j+l)}{2K}\right)\vartheta_4\left(\frac{\mathrm{i}(z_i-l)}{2K}\right)\vartheta_4\left(\frac{\mathrm{i}(\bar{z}_j-l)}{2K}\right)}.$$

Due to the symmetry relationship, the other two terms can be given by

$$\left[d_{14}(-x;z_i)d_{32}(-x;\bar{z}_j) - d_{14}(-x;\bar{z}_j)d_{32}(-x;z_i)\right] = \frac{\vartheta_3\left(\frac{2il}{2K}\right)\vartheta_4\left(\frac{kx}{2K}\right)\vartheta_1\left(\frac{\mathrm{i}(z_i-\bar{z}_j)}{2K}\right)\vartheta_2\left(\frac{\mathrm{i}(z_i+\bar{z}_j)-kx}{2K}\right)}{\vartheta_2\left(\frac{\mathrm{i}(z_i+l)}{2K}\right)\vartheta_2\left(\frac{\mathrm{i}(\bar{z}_j+l)}{2K}\right)\vartheta_4\left(\frac{\mathrm{i}(z_i-l)}{2K}\right)\vartheta_4\left(\frac{\mathrm{i}(\bar{z}_j-l)}{2K}\right)},$$

$$\left[d_{32}(x;z_i)d_{32}(-x;\bar{z}_j) - d_{14}(x;z_i)d_{14}(-x;\bar{z}_j)\right] = \frac{\vartheta_3\left(\frac{2il}{2K}\right)\vartheta_4\left(\frac{kx}{2K}\right)\vartheta_3\left(\frac{\mathrm{i}(z_i+\bar{z}_j)}{2K}\right)\vartheta_4\left(\frac{\mathrm{i}(z_i-\bar{z}_j)+kx}{2K}\right)}{\vartheta_2\left(\frac{\mathrm{i}(z_i+l)}{2K}\right)\vartheta_2\left(\frac{\mathrm{i}(\bar{z}_j+l)}{2K}\right)\vartheta_4\left(\frac{\mathrm{i}(z_i-l)}{2K}\right)\vartheta_4\left(\frac{\mathrm{i}(\bar{z}_j-l)}{2K}\right)}.$$

Similarly, by using the addition formula (see 3.8 of Ref. [37]) and according to the $\lambda(z)$ in Eq. (41), we arrive at

$$2\left(\lambda(z_i)-\lambda(\bar{z}_j)\right) = \mathrm{i}G(x)\frac{\vartheta_3\left(\frac{2il}{2K}\right)\vartheta_4\left(\frac{kx}{2K}\right)\vartheta_1\left(\frac{\mathrm{i}(z_i-\bar{z}_j)}{2K}\right)\vartheta_3\left(\frac{\mathrm{i}(z_i+\bar{z}_j)}{2K}\right)}{\vartheta_2\left(\frac{\mathrm{i}(z_i+l)}{2K}\right)\vartheta_2\left(\frac{\mathrm{i}(\bar{z}_j+l)}{2K}\right)\vartheta_4\left(\frac{\mathrm{i}(z_i-l)}{2K}\right)\vartheta_4\left(\frac{\mathrm{i}(\bar{z}_j-l)}{2K}\right)}. \tag{56}$$

Furthermore, we have

$$\mathbf{M}_{j,i} = \frac{\Psi^\dagger(z_j)\Psi(z_i)}{2\left(\lambda(z_i)-\lambda(\bar{z}_j)\right)} = -\mathrm{i}G(x)M_{j,i}, \tag{57}$$

where

$$M_{j,i} =\omega_2(x,t;z_i)\bar{\omega}_2(x,t;z_j)\frac{\vartheta_4\left(\frac{\mathrm{i}(z_i-\bar{z}_j)-kx}{2K}\right)}{\vartheta_1\left(\frac{\mathrm{i}(z_i-\bar{z}_j)}{2K}\right)}+\alpha_i\omega_1^{-1}(x,t)\omega_2^{-1}(x,t;z_i)\bar{\omega}_2(x,t;z_j)\frac{\vartheta_2\left(\frac{\mathrm{i}(z_i+\bar{z}_j)+kx}{2K}\right)}{\vartheta_3\left(\frac{\mathrm{i}(z_i+\bar{z}_j)}{2K}\right)}$$
$$+\bar{\alpha}_j\omega_1(x,t)\omega_2(x,t;z_i)\bar{\omega}_2^{-1}(x,t;z_j)\frac{\vartheta_2\left(\frac{\mathrm{i}(z_i+\bar{z}_j)-kx}{2K}\right)}{\vartheta_3\left(\frac{\mathrm{i}(z_i+\bar{z}_j)}{2K}\right)}+\alpha_i\bar{\alpha}_j\omega_2^{-1}(x,t;z_i)\bar{\omega}_2^{-1}(x,t;z_j)\frac{\vartheta_4\left(\frac{\mathrm{i}(z_i-\bar{z}_j)+kx}{2K}\right)}{\vartheta_1\left(\frac{\mathrm{i}(z_i-\bar{z}_j)}{2K}\right)}.$$

In addition, we also have

$$\Psi_1(z_i)\bar{\Psi}_2(z_j)=-\mathrm{i}G(x)^2\left(\omega_1^{-1}(x,t)\omega_2(x,t;z_i)\bar{\omega}_2(x,t;z_j)\frac{\vartheta_1\left(\frac{\mathrm{i}(z_i-l)-kx}{2K}\right)}{\vartheta_4\left(\frac{\mathrm{i}(z_i-l)}{2K}\right)}\frac{\vartheta_3\left(\frac{\mathrm{i}(\bar{z}_j+l)+kx}{2K}\right)}{\vartheta_2\left(\frac{\mathrm{i}(\bar{z}_j+l)}{2K}\right)}\right.$$
$$+\alpha_i\bar{\omega}_2(x,t;z_j)\omega_1^{-2}(x,t)\omega_2^{-1}(x,t;z_i)\frac{\vartheta_3\left(\frac{\mathrm{i}(z_i+l)+kx}{2K}\right)}{\vartheta_2\left(\frac{\mathrm{i}(z_i+l)}{2K}\right)}\frac{\vartheta_3\left(\frac{\mathrm{i}(\bar{z}_j+l)+kx}{2K}\right)}{\vartheta_2\left(\frac{\mathrm{i}(\bar{z}_j+l)}{2K}\right)}$$
$$-\bar{\alpha}_j\omega_2(x,t;z_i)\bar{\omega}_2^{-1}(x,t;z_j)\frac{\vartheta_1\left(\frac{\mathrm{i}(z_i-l)-kx}{2K}\right)}{\vartheta_4\left(\frac{\mathrm{i}(z_i-l)}{2K}\right)}\frac{\vartheta_1\left(\frac{\mathrm{i}(\bar{z}_j-l)-kx}{2K}\right)}{\vartheta_4\left(\frac{\mathrm{i}(\bar{z}_j-l)}{2K}\right)}$$
$$\left.-\alpha_i\bar{\alpha}_j\omega_1^{-1}(x,t)\omega_2^{-1}(x,t;z_i)\bar{\omega}_2^{-1}(x,t;z_j)\frac{\vartheta_1\left(\frac{\mathrm{i}(\bar{z}_j-l)-kx}{2K}\right)}{\vartheta_4\left(\frac{\mathrm{i}(\bar{z}_j-l)}{2K}\right)}\frac{\vartheta_3\left(\frac{\mathrm{i}(z_i+l)+kx}{2K}\right)}{\vartheta_2\left(\frac{\mathrm{i}(z_i+l)}{2K}\right)}\right). \tag{58}$$

Based on Eqs. (40), we note that $q(x,t)$ can be represented in the form:

$$q(x,t)=\omega_1^{-1}(x,t)G(x,t)\frac{\vartheta_2\left(\frac{kx+2\mathrm{i}l}{2K}\right)}{\vartheta_3\left(\frac{2\mathrm{i}l}{2K}\right)}. \tag{59}$$

With the above results and the additional formula for the theta functions (see 3.5b and 3.7 of Ref. [37]), the $\mathbf{H}_{j,i}$ in Eq. (54) can be written as

$$\mathbf{H}_{j,i}=q(x,t)\mathbf{M}_{j,i}-\bar{\Psi}_2(z_j)\Psi_1(z_i)=-\mathrm{i}\omega_1^{-1}(x,t)G^2(x,t)H_{j,i}, \tag{60}$$

where

$$H_{j,i} =\omega_2(x,t;z_i)\bar{\omega}_2(x,t;z_j)\frac{\vartheta_2\left(\frac{\mathrm{i}(z_i+l)}{2K}\right)\vartheta_2\left(\frac{\mathrm{i}(z_i-\bar{z}_j-2l)-kx}{2K}\right)\vartheta_4\left(\frac{kx}{2K}\right)\vartheta_4\left(\frac{\mathrm{i}(\bar{z}_j-l)}{2K}\right)}{\vartheta_1\left(\frac{\mathrm{i}(z_i-\bar{z}_j)}{2K}\right)\vartheta_2\left(\frac{\mathrm{i}(\bar{z}_j+l)}{2K}\right)\vartheta_3\left(\frac{2\mathrm{i}l}{2K}\right)\vartheta_4\left(\frac{\mathrm{i}(z_i-l)}{2K}\right)}$$
$$+\alpha_i\omega_1^{-1}(x,t)\omega_2^{-1}(x,t;z_i)\bar{\omega}_2(x,t;z_j)\frac{-\vartheta_4\left(\frac{\mathrm{i}(z_i-l)}{2K}\right)\vartheta_4\left(\frac{\mathrm{i}(z_i+\bar{z}_j+2l)+kx}{2K}\right)\vartheta_4\left(\frac{kx}{2K}\right)\vartheta_4\left(\frac{\mathrm{i}(\bar{z}_j-l)}{2K}\right)}{\vartheta_3\left(\frac{\mathrm{i}(z_i+\bar{z}_j)}{2K}\right)\vartheta_2\left(\frac{\mathrm{i}(\bar{z}_j+l)}{2K}\right)\vartheta_3\left(\frac{2\mathrm{i}l}{2K}\right)\vartheta_2\left(\frac{\mathrm{i}(z_i+l)}{2K}\right)}$$
$$+\bar{\alpha}_j\omega_1(x,t)\omega_2(x,t;z_i)\bar{\omega}_2^{-1}(x,t;z_j)\frac{\vartheta_2\left(\frac{\mathrm{i}(z_i+l)}{2K}\right)\vartheta_4\left(\frac{\mathrm{i}(z_i+\bar{z}_j-2l)-kx}{2K}\right)\vartheta_4\left(\frac{kx}{2K}\right)\vartheta_2\left(\frac{\mathrm{i}(\bar{z}_j+l)}{2K}\right)}{\vartheta_3\left(\frac{\mathrm{i}(z_i+\bar{z}_j)}{2K}\right)\vartheta_4\left(\frac{\mathrm{i}(\bar{z}_j-l)}{2K}\right)\vartheta_3\left(\frac{2\mathrm{i}l}{2K}\right)\vartheta_4\left(\frac{\mathrm{i}(z_i-l)}{2K}\right)}$$
$$+\alpha_i\bar{\alpha}_j\omega_2^{-1}(x,t;z_i)\bar{\omega}_2^{-1}(x,t;z_j)\frac{\vartheta_2\left(\frac{\mathrm{i}(\bar{z}_j+l)}{2K}\right)\vartheta_2\left(\frac{\mathrm{i}(z_i-\bar{z}_j+2l)+kx}{2K}\right)\vartheta_4\left(\frac{kx}{2K}\right)\vartheta_4\left(\frac{\mathrm{i}(z_i-l)}{2K}\right)}{\vartheta_1\left(\frac{\mathrm{i}(z_i-\bar{z}_j)}{2K}\right)\vartheta_2\left(\frac{\mathrm{i}(z_i+l)}{2K}\right)\vartheta_3\left(\frac{2\mathrm{i}l}{2K}\right)\vartheta_4\left(\frac{\mathrm{i}(\bar{z}_j-l)}{2K}\right)}.$$

Therefore, by inserting Eq. (57) and Eq. (60) into Eq. (54), we derive the multi-breather solutions of Eq. (1) on the background of the Jacobi elliptic functions

$$q_n(x,t) = q(x,t)\frac{\det\left(H_n\right)}{\det\left(M_n\right)}\left(\frac{\vartheta_3\left(\frac{2\mathrm{i}l}{2K}\right)}{\vartheta_2\left(\frac{kx+2\mathrm{i}l}{2K}\right)}\right)^n, \tag{61}$$

in which $H_n = (H_{j,i})_{1\le i,j\le n}$ and $M_n = (M_{j,i})_{1\le i,j\le n}$.

4.1. Breather solutions on the dn-periodic wave background

First, we consider the parameters $l = l_d = \frac{K'}{2}$ and $n = 1$ in Eq. (61), with which one can obtain a single breather solution on the dn-periodic wave. Furthermore, with the aid of the shift formula of theta functions (see 2.7 of Ref. [37]), we derive a more compact expression for the breather solution:

$$q_1 = k\frac{\vartheta_4}{\vartheta_3}\frac{H_d}{M_d}e^{2[\alpha s_2+\beta(3s_2^2-4s_4)]t}, \tag{62}$$

where

$$M_d = \frac{\vartheta_4\left(\frac{\mathrm{i}(z_1-\bar{z}_1)-kx}{2K}\right)}{\vartheta_1\left(\frac{\mathrm{i}(z_1-\bar{z}_1)}{2K}\right)} + \eta_1\frac{\vartheta_2\left(\frac{\mathrm{i}(z_1+\bar{z}_1)+kx}{2K}\right)}{\vartheta_3\left(\frac{\mathrm{i}(z_1+\bar{z}_1)}{2K}\right)} + \bar{\eta}_1\frac{\vartheta_2\left(\frac{\mathrm{i}(z_1+\bar{z}_1)-kx}{2K}\right)}{\vartheta_3\left(\frac{\mathrm{i}(z_1+\bar{z}_1)}{2K}\right)} + |\eta_1|^2\frac{\vartheta_4\left(\frac{\mathrm{i}(z_1-\bar{z}_1)+kx}{2K}\right)}{\vartheta_1\left(\frac{\mathrm{i}(z_1-\bar{z}_1)}{2K}\right)},$$

$$H_d = \frac{\eta_2}{\bar{\eta}_2}\frac{\vartheta_3\left(\frac{\mathrm{i}(z_1-\bar{z}_1)-kx}{2K}\right)}{\vartheta_1\left(\frac{\mathrm{i}(z_1-\bar{z}_1)}{2K}\right)} - \mathrm{i}\frac{\eta_1}{|\eta_2|^2}\frac{\vartheta_1\left(\frac{\mathrm{i}(z_1+\bar{z}_1)+kx}{2K}\right)}{\vartheta_3\left(\frac{\mathrm{i}(z_1+\bar{z}_1)}{2K}\right)} - \mathrm{i}\bar{\eta}_1|\eta_2|^2\frac{\vartheta_1\left(\frac{\mathrm{i}(z_1+\bar{z}_1)-kx}{2K}\right)}{\vartheta_3\left(\frac{\mathrm{i}(z_1+\bar{z}_1)}{2K}\right)} + |\eta_1|^2\frac{\bar{\eta}_2}{\eta_2}\frac{\vartheta_3\left(\frac{\mathrm{i}(z_1-\bar{z}_1)+kx}{2K}\right)}{\vartheta_1\left(\frac{\mathrm{i}(z_1-\bar{z}_1)}{2K}\right)},$$

and $\eta_1 = \alpha_1\exp\left(\varpi x - \varrho t\right)$,

$$\varpi = \left(\frac{\mathrm{i}\pi}{2K}k - 2Z(\mathrm{i}(z_1-l_d))k - 2\mathrm{i}\lambda\right), \quad \varrho = 2\mathrm{i}y\left(2\alpha+\beta(4s_2-8\lambda^2)\right), \quad \eta_2 = \frac{\vartheta_2\left(\frac{\mathrm{i}(z_1+l_d)}{2K}\right)}{\vartheta_4\left(\frac{\mathrm{i}(z_1-l_d)}{2K}\right)}\mathrm{e}^{\frac{-\pi z_1}{2K}},$$

$$\lambda = \frac{\mathrm{i}}{2}km^2\,\mathrm{sn}(\mathrm{i}(z_1-l_d))\,\mathrm{cd}(\mathrm{i}(z_1-l_d)), \quad y = \frac{1}{4}k^2m^2\left(\mathrm{sn}(\mathrm{i}(z_1-l_d))^2 - \mathrm{cd}(\mathrm{i}(z_1-l_d))^2\right).$$

Fixing the parameters of background solution $k = 1$ and $m = \frac{\sqrt{2}}{2}$, we have $u_1 = 0$, $u_2 = \frac{1}{2}$, $u_3 = 1$, $s_2 = \frac{3}{4}$ and $s_4 = \frac{1}{64}$. From Eq. (40), one can obtain that the maximum of $|q|$ located on these lines: $x = 2\tau K$, $\tau \in \mathbb{Z}$. And the maximum of $|q_1|$ can be calculated by the peak-height formula [15]: $|q_n| = |q| + \sum_{i=1}^{n} 2|\mathrm{Im}(\lambda(z_i))|$. To reveal the dynamic behaviors of the solution (62), we rewrite η_1 in this form:

$$\eta_1 = \alpha_1\left[2\exp\left(\frac{\xi_1}{2}\right)\cosh\left(\frac{\xi_1}{2}\right) - 1\right]\left[\cos(\xi_2) + \mathrm{i}\sin(\xi_2)\right], \quad \text{and} \quad \xi_1 = \varpi_R x - \varrho_R t, \quad \xi_2 = \varpi_I x - \varrho_I t, \tag{63}$$

where the subscript R and I represent the real and imaginary parts of the variable, respectively. In this way, we know that the breather is localized in the straight line: $\xi_1 = 0$.

For $\varpi_R \neq 0$, the velocity of the breather moving along the above line can be derived: $v = \varrho_R/\varpi_R$. By taking $z_1 = -0.6180 - 0.6953\mathrm{i}$ and $\alpha_1 = -1$, we plot the Fig. 1(a). It can be seen that the peaks all lie on a line, and the velocity is $v_1 = -7.1465$. Meanwhile, using the inverse of the velocity, the slopes of this line can be calculated: $K_1 = -0.1399$. Moreover, due to $\lambda(z_1) = 0.1526 + 0.7803\mathrm{i}$ and based on the peak-height formula, we obtain the maximum of $|q_1|$ is $1 + 2|\mathrm{Im}(\lambda(z_1))| = 2.5605$ located at the origin. Specially, we consider the choice $z_1 = -0.9270 - 0.6953\mathrm{i}$ such that $\varrho_R = 0$. This condition can result in a breather solution, which will propagate in the line: $x = 0$. On account of $\varrho_I = 3.1976$ and $\lambda(z_1) = 0.9229\mathrm{i}$, the period of breather in this line is $T = 2\pi/\varrho_I = 1.9650$, and the maximum of $|q_1|$ is 2.8458 located at $x = 0$ and

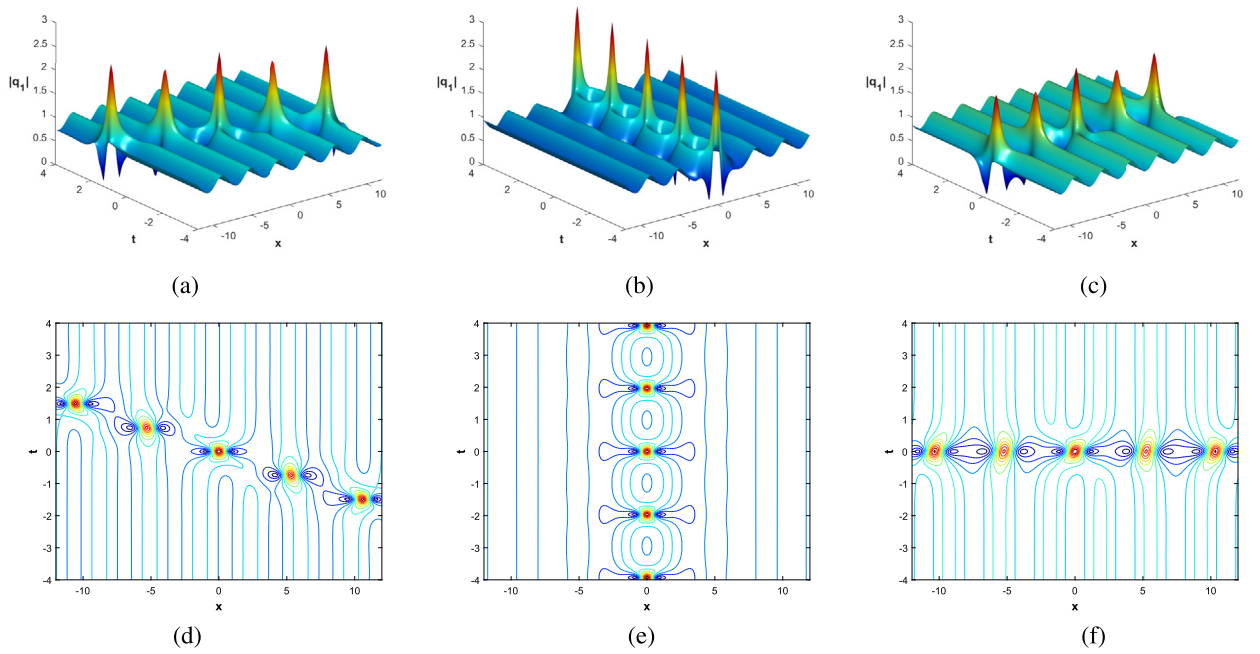

Fig. 1. The breather solutions of Eq. (1) with $\alpha = \beta = 1$ on the dn-periodic wave background. (a) The general breather (GB) solution with $z_1 = -0.6180 - 0.6953\mathrm{i}$ and $\alpha_1 = -1$. (b) The KMB solution with $z_1 = -0.9270 - 0.6953\mathrm{i}$ and $\alpha_1 = -1$. (c) The AB solution with $z_1 = -0.4000 - 0.9270\mathrm{i}$ and $\alpha_1 = -1$. (d-f) Show the contour plots of the corresponding solutions.

$t = \tau T$. To illustrate this point, we plot Fig. 1(b), it is shown that the solution is temporally breathing and spatially localized, which is similar to the KMB on the plane wave background.

On the other hand, by taking $z_1 = -0.4000 - 0.9270\mathrm{i}$ such that $\varpi_R = 0$, we can obtain another form of breather solution: the AB solution, and all its peaks located on the line: $t = 0$ as shown in Fig. 1(c). As seen from this figure, we find that the breather does not have a shift of crest, and the maximum value is 2.2064 located at the origin.

Next, by choosing the parameters $l = l_d$ and $n = 2$ in Eq. (61), we obtain two-breather solution on the dn-periodic wave background. Then, we fix the same parameters as the background wave in single breather solution. Taking $z_1 = -0.9270 - 0.6953\mathrm{i}$, $z_2 = -0.4000 - 0.9270\mathrm{i}$ and $\alpha_1 = \alpha_2 = -1$, we plot the Fig. 2(a). In this figure, it exhibits the spatio-temporal structure of an interaction between an AB and a KMB. Both breathers have no the shift of crest after the interaction. The maximum value can be derived by: $|q_2| = 1 + 2\mathrm{Im}(\lambda(z_1) + \lambda(z_2)) = 4.4063$, and it is also located at the origin. We note that at the crossing point there exists a fundamental second-order rogue wave with a "four-claw" symmetric structure around the central peak.

4.2. Breather solutions on the cn-periodic wave background

Similarly, by choosing the parameters $l = l_c = 0$ and $n = 1$ in Eq. (61), we can obtain the single breather solution on the cn-periodic wave background. Then, we fix the parameters of background solution $k = 1$ and $m = \frac{\sqrt{2}}{2}$, so that $u_1 = -\frac{1}{2}$, $u_2 = 0$, $u_3 = \frac{1}{2}$, $s_2 = \frac{3}{4}$ and $s_4 = \frac{1}{16}$. By taking $z_1 = -1.4833 + 0.4635\mathrm{i}$ and $\alpha_1 = 1$, we have $\lambda(z_1) = -1.4833 + 0.4635\mathrm{i}$ and plot the Fig. 3(a). It is shown that this solution is a GB moving to left along a line with the velocity -5.5744. The slope of this line is -0.1794 and the maximum amplitude of the breather is 1.9270 at the origin. In addition, if we take $z_1 = 1.8541 + 0.6953\mathrm{i}$, so that $y_1 = 3.2891$ and $\lambda(z_1) = -0.7024\mathrm{i}$, the KMB on the cn-periodic background can be obtained. As shown in Fig. 3(b), the breather is temporally breathing and spatially localized. By a calculation, we find that the period T is 0.9551 and the maximum value is 2.4048 at $x = 0$, $t = 2\tau T$. Moreover, by choosing

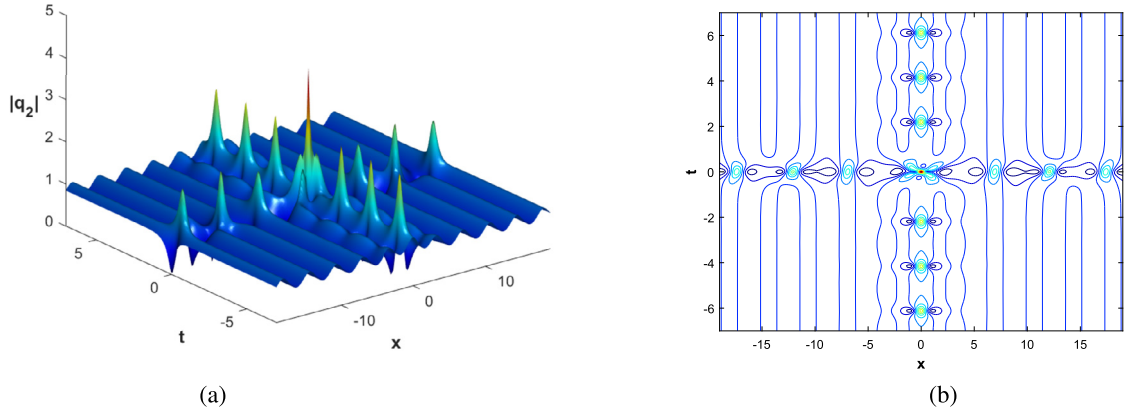

Fig. 2. (a) The two-breather solution of Eq. (1) on the dn-periodic wave background. (b) Show the contour plot of the solution. The parameters of the solution (62) are chosen as $\alpha = \beta = 1$, $z_1 = -0.9270 - 0.6953\mathrm{i}$, $z_2 = -0.4000 - 0.9270\mathrm{i}$ and $\alpha_1 = \alpha_2 = -1$.

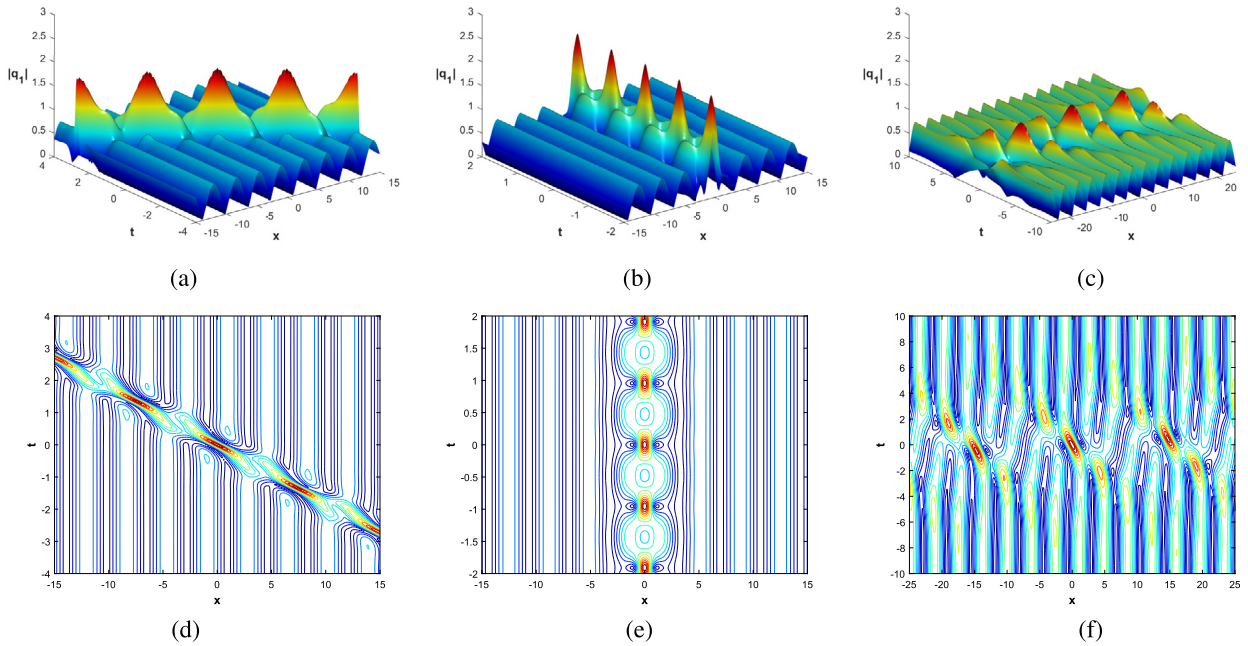

Fig. 3. The breather solutions of Eq. (1) with $\alpha = \beta = 1$ on the cn-periodic wave background. (a) The GB solution with $z_1 = -1.4833 + 0.4635\mathrm{i}$ and $\alpha_1 = 1$. (b) The KMB solution with $z_1 = -0.9270 - 0.6953\mathrm{i}$ and $\alpha_1 = 1$. (c) The AB solution with $z_1 = -0.4000 - 0.9270\mathrm{i}$ and $\alpha_1 = -1$. (d-f) Show the contour plots of the corresponding solutions.

$z_1 = -0.7711 - 0.56\mathrm{i}$ and $\alpha_1 = -1$, we can obtain the AB on the cn-periodic background, as shown in Fig. 3(c). From this figure, we deduce that the breather admits the shift of crest, and the maximum value is 1.2643 at the origin.

Next, by taking the parameters $l = l_c$ and $n = 2$ in Eq. (61), the two-breather solution on the cn-periodic wave background can be obtained. Taking $z_1 = -1.4833 + 0.4635\mathrm{i}$, $z_2 = -0.7711 - 0.56\mathrm{i}$ and $\alpha_1 = \alpha_2 = 1$, we plot the Fig. 4(a). From this figure, we can see that this solution exhibits an interaction between a GB and a KMB. Two breathers both have the shift of crest after the interaction.

5. Rogue waves on the elliptic function background

In the previous section, we know that the period of breather solutions (KMB solution or AB solution) is related to $y(\lambda)$ (i.e., $T = 2\pi/\varrho_I$, $\varrho_I = \mathrm{Im}(2\mathrm{i}y(2\alpha + \beta(4s_2 - 8\lambda^2))))$. In the following, by taking $y(\lambda) \to 0$,

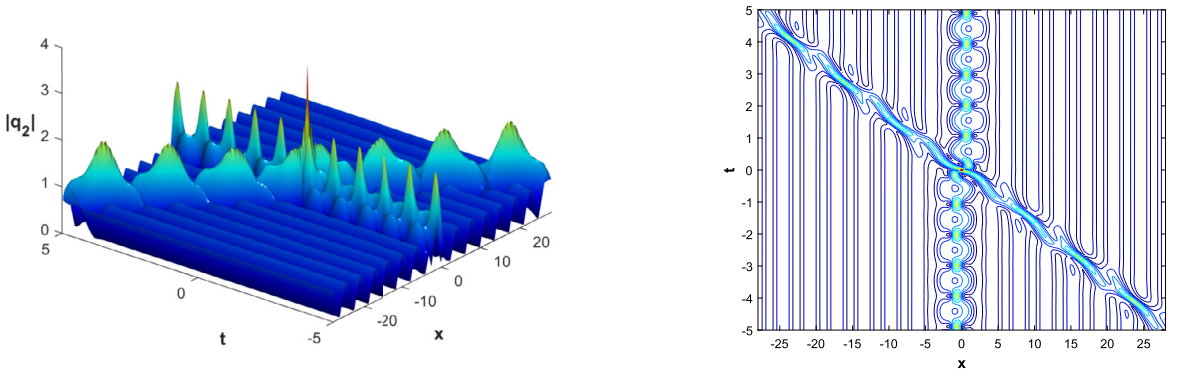

(a) (b)

Fig. 4. (a) The two-breather solution of Eq. (1) on the cn-periodic wave background. (b) Show the contour plot of the solution. The parameters of the solution (61) are chosen as $\alpha = \beta = 1$, $z_1 = -1.4833 + 0.4635\mathrm{i}$, $z_2 = 1.4833 + 0.4635\mathrm{i}$ and $\alpha_1 = \alpha_2 = 1$.

we will construct rogue wave solutions on the elliptic function background. To begin with, we expand the parameter $y(\lambda)$ at the branch point $\lambda_1 : \lambda = \lambda_1 + \epsilon_1^2$ with ϵ_1 being small parameter, and we arrive at

$$y(\lambda) = \sqrt{(\lambda-\lambda_1)(\lambda-\lambda_2)(\lambda-\lambda_3)(\lambda-\lambda_4)} = \epsilon_1 y_1 Y_1, \tag{64}$$

where

$$y_1 = \sqrt{(\lambda_1-\lambda_2)(\lambda_1-\lambda_3)(\lambda_1-\lambda_4)}, \quad Y_1 = \sqrt{\left(1+\frac{\epsilon_1^2}{\lambda_1-\lambda_2}\right)\left(1+\frac{\epsilon_1^2}{\lambda_1-\lambda_3}\right)\left(1+\frac{\epsilon_1^2}{\lambda_1-\lambda_4}\right)}.$$

Furthermore, we have

$$\begin{aligned}
&\gamma_1 = \lambda_1^2 + s_2/2 + \epsilon_1^2(2\lambda_1+\epsilon_1^2) - \epsilon_1 y_1 Y_1, \quad u(x) - 2\gamma_1 = u_1(x) - 2\epsilon^2\left(2\lambda_1+\epsilon_1^2\right) + 2\epsilon_1 y_1 Y_1,\\
&C_1 = C_0 + 4\left[\epsilon_1^2(3\lambda_1^2 + s_2/2 + 3\lambda_1\epsilon_1^2 + \epsilon_1^4) - \epsilon_1 y_1 Y_1(\lambda_1+\epsilon_1^2)\right],\\
&D_1 = \varrho_0 + \epsilon_1 y_1 Y_1\left[\varrho_1 - 8\beta\epsilon_1^2(2\lambda_1+\epsilon_1^2)\right],
\end{aligned}$$

in which $u_1(x) = u(x) - \left(2\lambda_1^2 + s_2\right)$, $C_0 = 4\lambda_1^3 + 2s_2\lambda_1$, $\varrho_0 = \alpha s_2 + \beta(3s_2^2 - 4s_4)$ and $\varrho_1 = 2\alpha + \beta(4s_2 - 8\lambda_1^2)$. Then, by inserting the above equations into the vector solution Ψ_1, we would like to expand them in Taylor series of ϵ_1. In this way, we first consider the expansion of ψ_1 as follows:

$$\psi_1 = \sqrt{u(x) - 2\gamma_1}\exp(\theta_1) = \sum_{i=0}^{\infty}\psi_1^{[i]}\epsilon_1^{[i]}, \quad \theta_1 = \mathrm{i}\int_0^x \frac{C_1\,\mathrm{d}s}{u(s)-2\gamma_1} + \mathrm{i}\lambda x + \mathrm{i}D_1 t. \tag{65}$$

Then, with the aid of Eqs. (5), (10) and (22), we arrive at

$$\phi_1 = \frac{\mathrm{i}h}{f-y}\psi_1 = \frac{2u(x)\lambda - \mathrm{i}u_x(x)/2}{\sqrt{u(x)}\sqrt{u(x)-2\gamma_1}}\exp(\theta_1-\theta_0) = \sum_{i=0}^{\infty}\phi_1^{[i]}\epsilon_1^{[i]}, \tag{66}$$

where $\theta_0 = 2\mathrm{i}\varrho_0 t$ and the above expansion coefficients $\psi_1^{[i]}$ and $\phi_1^{[i]}$ are defined by

$$\psi_1^{[i]} = \frac{1}{i!}\frac{\partial^i\psi_1}{\partial\epsilon_1^i}|_{\epsilon_1=0}, \quad \phi_1^{[i]} = \frac{1}{i!}\frac{\partial^i\phi_1}{\partial\epsilon_1^i}|_{\epsilon_1=0}.$$

In a similar procedure, ψ_2 and ϕ_2 can be treated for the other eigenvalue $\lambda = \lambda_2 + \epsilon_2^2$ with ϵ_2 as a small parameter

$$\psi_2 = \sum_{i=0}^{\infty} \psi_2^{[i]} \epsilon_2^{[i]}, \quad \phi_2 = \sum_{i=0}^{\infty} \phi_2^{[i]} \epsilon_2^{[i]}, \tag{67}$$

where $\psi_2^{[i]}$ and $\phi_2^{[i]}$ have the same forms of $\psi_1^{[i]}$ and $\phi_1^{[i]}$ by exchanging λ_1 to λ_2. Moreover, using Eq. (10) and $f^2 - gh = 0$, we have

$$u_1(x)^2 = -\frac{1}{u(x)} \left[\left(2u(x)\lambda_1 - \frac{\mathrm{i}u_x(x)}{2} \right) \left(2u(x)\lambda_1 + \frac{\mathrm{i}u_x(x)}{2} \right) \right]. \tag{68}$$

To avoid singularity, we consider a different representation for the expansion coefficients of ϕ_1 based on Eq. (68). For convenience, we would present the first two odd-order coefficients

$$\psi_1^{[1]} = \frac{r_1(x)}{\sqrt{u_1(x)}} \exp(\Theta_1), \quad \phi_1^{[1]} = -\frac{r_2(x)\sqrt{u(x)u_1(x)}}{J_1(x)} \exp(\Theta_2), \tag{69}$$

$$\psi_1^{[3]} = \frac{\sum_{i=1}^{4} (e_{i1}\xi_i) + e_{01}}{6\sqrt{u_1(x)}} \exp(\Theta_1), \quad \phi_1^{[3]} = \sqrt{u(x)u_1(x)} \left[\frac{2r_2(x)}{u_1(x)^2} - \frac{\sum_{i=1}^{4} (e_{i2}\xi_i) + e_{02}}{6J_1(x)} \right] \exp(\Theta_2), \tag{70}$$

with

$$\begin{aligned}
&\Theta_1 = \mathrm{i}C_0\xi_1 + \mathrm{i}\lambda_1 x + \mathrm{i}\varrho_0 t, \quad \Theta_2 = \Theta_1 - 2\mathrm{i}\varrho_0 t, \quad J_1(x) = 2u(x)\lambda_1 + \frac{\mathrm{i}u_x(x)}{2}, \\
&r_1(x) = 1 + \left(\mathrm{i}\varrho_1 t - 4\mathrm{i}\lambda_1 \left(\xi_1 + (2\lambda_1^2 + s_2)\xi_2 \right) \right) u_1(x), \quad r_2(x) = r_1(x) - 2, \\
&e_{0j} = 3r_j(x) \left(\sum_{i=2}^{4} \frac{1}{\lambda_1 - \lambda_i} + 2\mathrm{i}x \right) \pm \frac{12\lambda_1}{u_1(x)} \left(2 - r_j(x) \right) + \frac{y_1^2}{u_1(x)^2} \left(r_j(x)^3 \pm (8 - 6r_j(x)) \right), \\
&e_{1j} = 12\mathrm{i} \left(s_2 r_j(x) + 6\lambda_1^2 r_j(x) - 2u_1(x) \right), e_{4j} = -96\mathrm{i}\lambda_1 y_1^2 \left(2\lambda_1^2 + s_2 \right) u_1(x), \\
&e_{3j} = 48\mathrm{i}\lambda_1 \left(y_1^2 \left(s_2 r_j(x) + 2\lambda_1^2 r_j(x) - 2u_1(x) \right) - 4\lambda_1 \left(2\lambda_1^2 + s_2 \right) u_1(x) \right), \\
&e_{2j} = 24\mathrm{i} \left(s_2 \left(2\lambda_1^2 r_j(x) - u_1(x) \right) + 2\lambda_1 \left(-5\lambda_1 u_1(x) + 2\lambda_1^3 r_j(x) + y_1^2 r_j(x) \right) \right),
\end{aligned}$$

in which $j = 1, 2$, and the definition of ξ_i is given by

$$\xi_i := \int_0^x \frac{\mathrm{d}s}{u_1(s)^i} = \kappa^i \int_0^x \frac{\mathrm{d}s}{\left(1 - \zeta^2 \mathrm{sn}^2(s)\right)^i}, \quad \kappa = \frac{1}{u_3 - (2\lambda_1^2 + s_2)}, \quad \zeta^2 = \frac{u_3 - u_2}{u_3 - (2\lambda_1^2 + s_2)}. \tag{71}$$

To calculate ξ_i, we would use the integration formulas (see 336 of Ref. [9]) of Jacobi elliptic functions, and obtain

$$\xi_1 = \kappa \Pi(\varphi, \zeta^2, m), \quad \varphi = \mathrm{am}(kx), \tag{71a}$$

$$\xi_2 = \frac{\kappa^2}{2(1-\zeta^2)(m^2-\zeta^2)} \left[-\zeta^2 E(kx) + (\zeta^2 - m^2)kx - \frac{1}{\kappa}\upsilon_1\xi_1 + \frac{\zeta^4 \mathrm{sn}(kx)\mathrm{cn}(kx)\mathrm{dn}(kx)}{1 - \zeta^2 \mathrm{sn}(kx)} \right], \tag{71b}$$

$$\xi_3 = \frac{\kappa^3}{4(1-\zeta^2)(m^2-\zeta^2)} \left[m^2 kx + \frac{2}{\kappa}(m^2\zeta^2 + \zeta^2 - 3m^2)\xi_1 - \frac{3}{\kappa^2}\upsilon_1\xi_2 + \frac{\zeta^4 \mathrm{sn}(kx)\mathrm{cn}(kx)\mathrm{dn}(kx)}{(1 - \zeta^2 \mathrm{sn}(kx))^2} \right], \tag{71c}$$

$$\xi_4 = \frac{\kappa^4}{6(1-\zeta^2)(m^2-\zeta^2)}\left[\frac{3}{\kappa}m^2\xi_1 + \frac{4}{\kappa^2}(m^2\zeta^2+\zeta^2-3m^2)\xi_2 - \frac{5}{\kappa^3}\upsilon_1\xi_3 + \frac{\zeta^4 \mathrm{sn}(kx)\mathrm{cn}(kx)\mathrm{dn}(kx)}{(1-\zeta^2\mathrm{sn}(kx))^3}\right], \tag{71d}$$

where $\upsilon_1 = (2\zeta^2(1+m^2) - \zeta^4 - 3m^2)$, $E(kx)$ and $\Pi(\varphi, \zeta^2, m)$ respectively stand for the elliptic integral of the second and third kind (see appendix B of Ref. [63]), which can be given by

$$\begin{aligned} E(kx) &= Z(kx) + \frac{E(m)}{K(m)}kx, \\ \Pi\left(\varphi, \zeta^2, m\right) &= kx + \mathrm{sc}(\upsilon_2)\ \mathrm{nd}\ (\upsilon_2)\left(\frac{1}{2}\ln\frac{\vartheta_4\left(\frac{kx-\upsilon_2}{2K}\right)}{\vartheta_4\left(\frac{kx+\upsilon_2}{2K}\right)} + kxZ(\upsilon_2)\right), \quad \mathrm{sn}(\upsilon_2) = \frac{\zeta}{m}. \end{aligned} \tag{73}$$

Therefore, with the these Eqs. (71a)-(71d) and (73), we can obtain $\psi_j^{[i]}$ and $\phi_j^{[i]}$ to construct higher-order rogue wave solutions on the elliptic function background.

5.1. Rogue waves on the dn-periodic background

In this case, taking $\lambda_1 = \bar{\lambda}_3 = c\mathrm{i}$ and $\lambda_2 = \bar{\lambda}_4 = d\mathrm{i}$, then we fix the background solution $q(x,t) = k\,\mathrm{dn}\,(kx;m)\exp(\mathrm{i}at)$ with $k = c+d$, $m = \sqrt{\frac{4cd}{(c+d)^2}}$ and $a = 2\varrho_0 = 2[\alpha(c^2+d^2) + \beta(3c^4+2c^2d^2+3d^4)]$. To obtain the first-order rogue wave solution, we first derive $r_1(x)$ by using Eqs. (71a) and Eq. (71b)

$$\begin{aligned} r_1(x) &= 1 + \left(\mathrm{i}\varrho_1 t - 4\mathrm{i}\lambda_1\left(\xi_1 + (2\lambda_1^2+s_2)\xi_2\right)\right)u_1(x) \\ &= 1 + \left(\mathrm{i}\varrho_1 t + \frac{c+d}{2c(c-d)}\left(Z(kx) + \frac{E(m)}{K(m)}kx\right) + \frac{x}{2c}\right)u_1(x) - \frac{2d(c+d)}{c-d}\mathrm{sn}(kx)\mathrm{cn}(kx)\mathrm{dn}(kx), \end{aligned}$$

where $\varrho_1 = 2\alpha + 4\beta(3c^2+d^2)$, $u_1(x) = u(x) + c^2 - d^2$ and $u(x) = k^2\,\mathrm{dn}(kx)^2$. Next, taking $\psi_1 = \psi_1^{[1]}$ and $\phi_1 = \phi_1^{[1]}$ into one-fold DT (3), we obtain the first-order rogue wave solution on the dn-periodic background

$$q_1 = k\,\mathrm{dn}\,(kx;m)\left[1 + \frac{2cu_1(x)(|r_1(x,t)|^2 - 2r_1(x,t))(2\mathrm{ci}u(x) + \mathrm{i}u_x(x)/2)}{|r_1(x,t)|^2|2\mathrm{ci}u(x) + \mathrm{i}u_x(x)/2|^2 + u(x)u_1(x)^2|r_1(x,t)-2|^2}\right]\mathrm{e}^{\mathrm{i}at}. \tag{74}$$

It should be noted that another rogue wave solution can be derived by the interchange of the parameters c and d, which corresponds to a different branch point.

By choosing the amplitude of background wave as a fixed value $k = 1$, we plot Fig. 5(a) and Fig. 5(b). They exhibit the spatiotemporal patterns of two types of rogue waves on the background of the dn-periodic traveling wave, respectively. As seen from Fig. 5(a), the central part resembles an interaction between two solitons, and they collide elastically and generate a transient high wave in the interaction region. Fig. 5(b) displays a periodic oscillation of the rogue wave along the x-direction on the periodic background.

To continue, taking $\Psi_1 = (\psi_1^{[1]}, \phi_1^{[1]})^T$ and $\Psi_2 = (\psi_2^{[1]}, \phi_2^{[1]})^T$ into the two-fold DT (3), we can derive the second-order rogue wave solution on the periodic background

$$q_2 = k\,\mathrm{dn}(kx)\left[\frac{\det(\mathbf{H}_2)}{\det(\mathbf{M}_2)}\right]\mathrm{e}^{\mathrm{i}at}, \tag{75}$$

where

$$\mathbf{M}_2 = \begin{bmatrix} \frac{|\psi_1^{[1]}|^2 + |\phi_1^{[1]}|^2}{2c} & \frac{\bar{\psi}_1^{[1]}\psi_2^{[1]} + \bar{\phi}_1^{[1]}\phi_2^{[1]}}{c+d} \\ \frac{\bar{\psi}_2^{[1]}\psi_1^{[1]} + \bar{\phi}_2^{[1]}\phi_1^{[1]}}{c+d} & \frac{|\psi_2^{[1]}|^2 + |\phi_2^{[1]}|^2}{2d} \end{bmatrix}, \quad \mathbf{H}_2 = \mathbf{M}_2 - \frac{2\mathrm{i}\,\mathrm{e}^{-\mathrm{i}at}}{k\,\mathrm{dn}(kx)}\begin{bmatrix} \bar{\phi}_1^{[1]} \\ \bar{\phi}_2^{[1]} \end{bmatrix}\left[\psi_1^{[1]}, \psi_1^{[1]}\right],$$

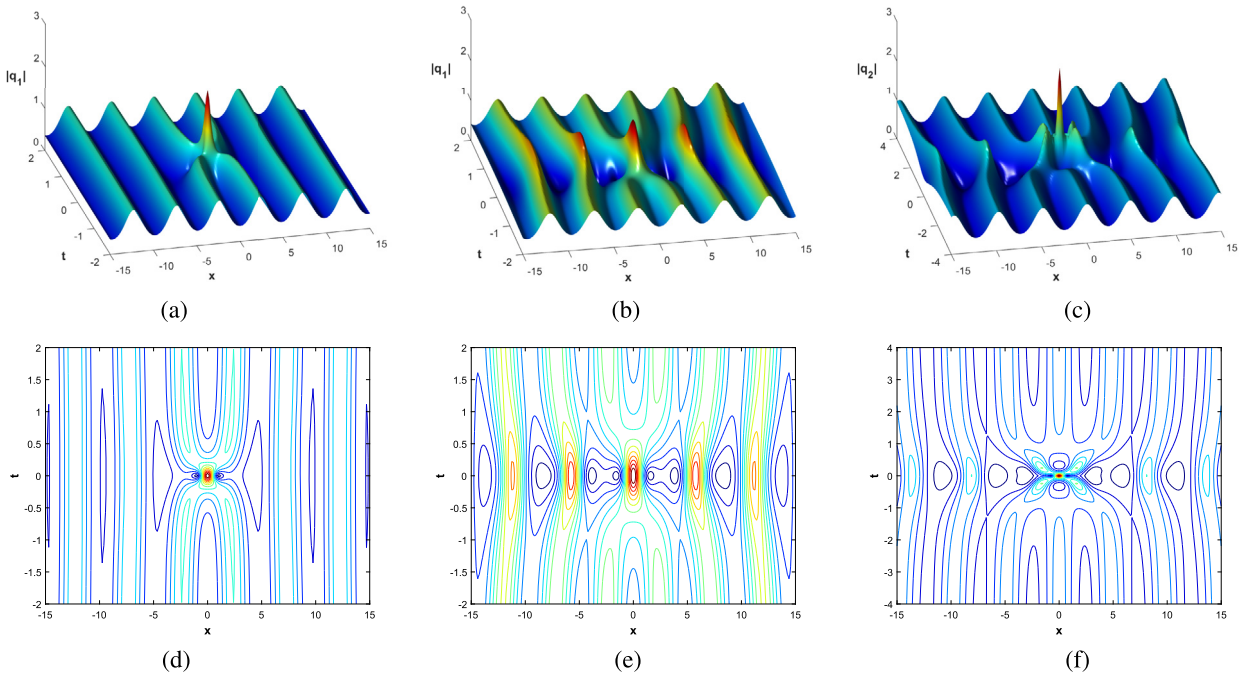

Fig. 5. (a) The first-order dn-rogue wave solution with $\alpha = \beta = 1$, $c = 0.675$, $d = 0.325$ and $m = 0.9367$. (b) The other first-order dn-rogue wave solution with $\alpha = \beta = 1$, $c = 0.325$, $d = 0.675$ and $m = 0.9367$. (c) The second-order dn-rogue wave solution. (d-f) Show the contour plots of the corresponding solutions.

in which $\psi_j^{[1]}$ and $\phi_j^{[1]}$ are given by Eq. (69).

By choosing the same parameters c and d as those in Fig. 5(b), we plot the Fig. 5(c), which shows the solution (75) on the dn-periodic wave. The maximum value of the $|q_2|$ is 3 at origin. It is observed that in the central part three solitons form a second-order rogue wave with a large peak, and the other part is still period in x.

Next, we give some special cases for the above rogue wave solutions. When $c \to 0$ and $d \to 1$ (or $d \to 0$ and $c \to 1$) such that $k = 1$, then we have $\mathrm{dn}(x; 0) = 1$. In this case, the rogue wave solution (74) can reduce to the classical rogue wave solution (Peregrine soliton) on the constant background. In Fig. 6(a), the maximum value of $|q_1|$ is about 3 at the origin. The maximum amplitude for the rogue wave is three times as that of the exciting plane wave. When $c \to d$, then $\mathrm{dn}(x; 1) = \mathrm{sech}(x)$, one can obtain that the rogue wave solutions (74) and (75) respectively reduce to the double- and third-pole soliton solutions, as shown in Fig. 6(b) and Fig. 6(c). The maximum values of $|q_1|$ and $|q_2|$ are 2 and 3 at the origin. In Fig. 6(b), two solitons with equal amplitudes elastically collide along with a strong interaction, and generate a first-order rogue wave. In Fig. 6(c), three solitons with equal amplitudes elastically collide and generate a second-order rogue wave. We would like to point out that this kind of multi-pole soliton solution was first reported by Zakharov and Shabat in the NLS equation [69]. The multi-pole solution can be regarded as the degeneration of the N-soliton solution when N distinct poles (reflection coefficient admits N simple poles in the terminology of the inverse scattering transform) coalesce into one.

In order to obtain higher-order rogue waves, we consider expansions at two different spectral parameters and take $m_1 = m_2 = 2$ in the generalized DT (4), then the corresponding second-second-fold potential transformation is represented as

$$q_{2,2} = q - 2\mathbf{X}_1\mathbf{M}^{-1}\mathbf{X}_2^{\dagger}, \tag{76}$$

where $\mathbf{M} = \mathbf{Y}\mathbf{S}\mathbf{Y}^{\dagger}$, $\mathbf{X} = [\Psi_1^{[0]}, \Psi_1^{[1]}, \Psi_2^{[0]}, \Psi_2^{[1]}]$ and

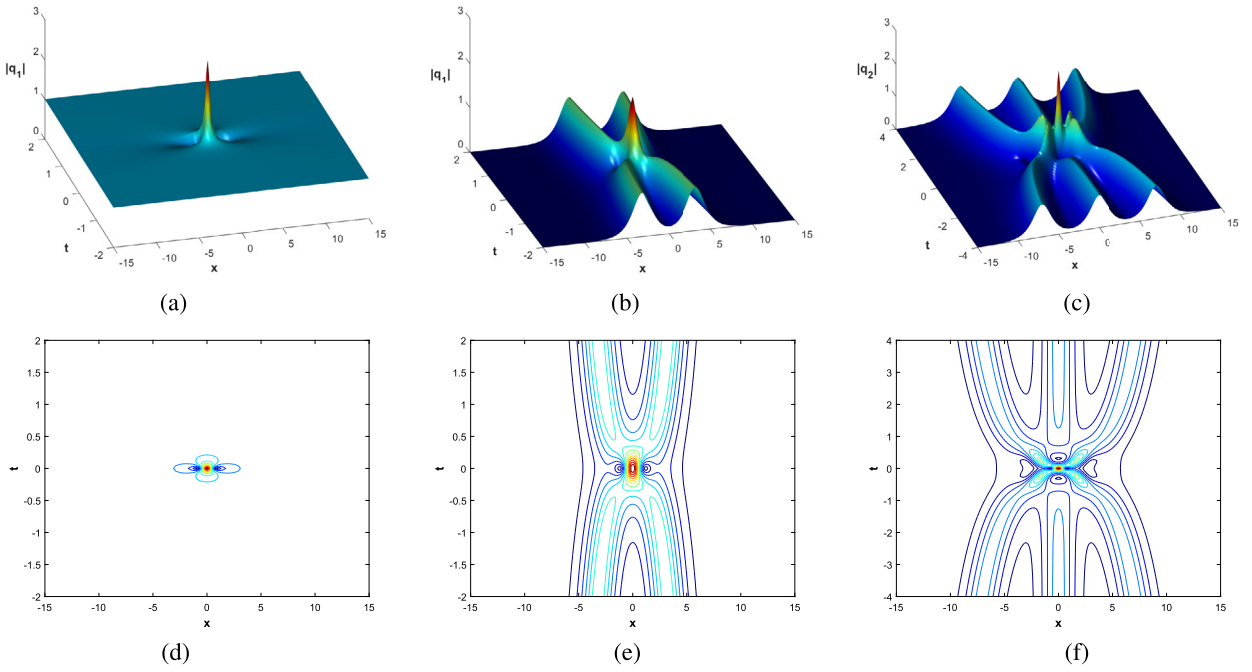

Fig. 6. (a) The Peregrine soliton via solution (74) with $c = 1$, $d = 0$ and $m = 0$. (b-c) The double- and third-pole soliton solutions (74) and (75) with $c = d = 0.5$ and $m = 1$. (d-f) Show the contour plots of the corresponding solutions.

$$\mathbf{Y} = \begin{bmatrix} \Psi_1^{[0]\dagger} & 0 & 0 & 0 \\ \Psi_1^{[1]\dagger} & \Psi_1^{[0]\dagger} & 0 & 0 \\ 0 & 0 & \Psi_2^{[0]\dagger} & 0 \\ 0 & 0 & \Psi_2^{[1]\dagger} & \Psi_2^{[0]\dagger} \end{bmatrix}, \quad \mathbf{S} = \begin{bmatrix} \frac{1}{\lambda_1-\bar{\lambda}_1} & \frac{-1}{(\lambda_1-\bar{\lambda}_1)^2} & \frac{1}{\lambda_2-\bar{\lambda}_1} & \frac{-1}{(\lambda_2-\bar{\lambda}_1)^2} \\ \frac{1}{(\lambda_1-\bar{\lambda}_1)^2} & \frac{-2}{(\lambda_1-\bar{\lambda}_1)^3} & \frac{1}{(\lambda_2-\bar{\lambda}_1)^2} & \frac{-2}{(\lambda_2-\bar{\lambda}_1)^3} \\ \frac{1}{\lambda_1-\bar{\lambda}_2} & \frac{-1}{(\lambda_1-\bar{\lambda}_2)^2} & \frac{1}{\lambda_2-\bar{\lambda}_2} & \frac{-1}{(\lambda_2-\bar{\lambda}_2)^2} \\ \frac{1}{(\lambda_1-\bar{\lambda}_2)^2} & \frac{-2}{(\lambda_1-\bar{\lambda}_2)^3} & \frac{1}{(\lambda_2-\bar{\lambda}_2)^2} & \frac{-2}{(\lambda_2-\bar{\lambda}_2)^3} \end{bmatrix}.$$

Taking $\Psi_j^{[0]} = (\psi_j^{[1]}, \phi_j^{[1]})^T$ and $\Psi_j^{[1]} = (\psi_j^{[3]}, \phi_j^{[3]})^T$, and plugging them into Eq. (76), thus we can obtain the second-second-order rogue wave solution.

By setting the parameters $c = 0.675$ and $d = 0.325$, we can obtain the second-second-order rogue wave on the dn-periodic background. As shown in Fig. 7, it is clearly seen that a larger-amplitude rogue wave is located at the origin, which corresponds to the third-pole soliton solution on the dn-periodic background. The rogue wave shown in Fig. 7 is actually enhanced in the center position up to 5 times as high as the height of the periodic background. In fact, we can compute the maximum value formulas: $|q_{2,2}| = |q(x,t)| + 2|2\mathrm{Im}(\lambda_1)| + 2|2\mathrm{Im}(\lambda_2)|$.

5.2. Rogue waves on the cn-periodic background

Similarly, the parameter choices are $\lambda_1 = \bar{\lambda}_3 = b + d\mathrm{i}$ and $\lambda_2 = \bar{\lambda}_4 = -b + d\mathrm{i}$, then we fix the background solution $q(x,t) = km\,\mathrm{cn}\,(kx;m)\exp(\mathrm{i}at)$ with $k = 2\sqrt{b^2+d^2}$, $m = \sqrt{\frac{d^2}{b^2+d^2}}$ and $a = 4[\alpha(d^2-b^2) + 4\beta(b^4 - 4b^2d^2 + d^4)]$. To continue, we first give $r_1(x)$ in the form

$$r_1(x) = 1 + \left(\mathrm{i}\varrho_1 t + \frac{-b+d\mathrm{i}}{2bc}\left(Z(kx) + \frac{E(m)}{K(m)}kx\right) + \frac{x}{2c}\right)u_1(x) + \frac{2d(-b+d\mathrm{i})}{b}\mathrm{sn}(kx)\mathrm{cn}(kx)\mathrm{dn}(kx),$$

where $\varrho_1 = 2\alpha + 16\beta(d^2 - b^2 + bd\mathrm{i})$, $u_1(x) = u(x) + 4bd\mathrm{i}$ and $u(x) = k^2m^2\,\mathrm{cn}(kx)^2$. Then, taking $\psi_1 = \psi_1^{[1]}$ and $\phi_1 = \phi_1^{[1]}$, and inserting them into one-fold DT (3), thus we can derive the first-order rogue wave solution.

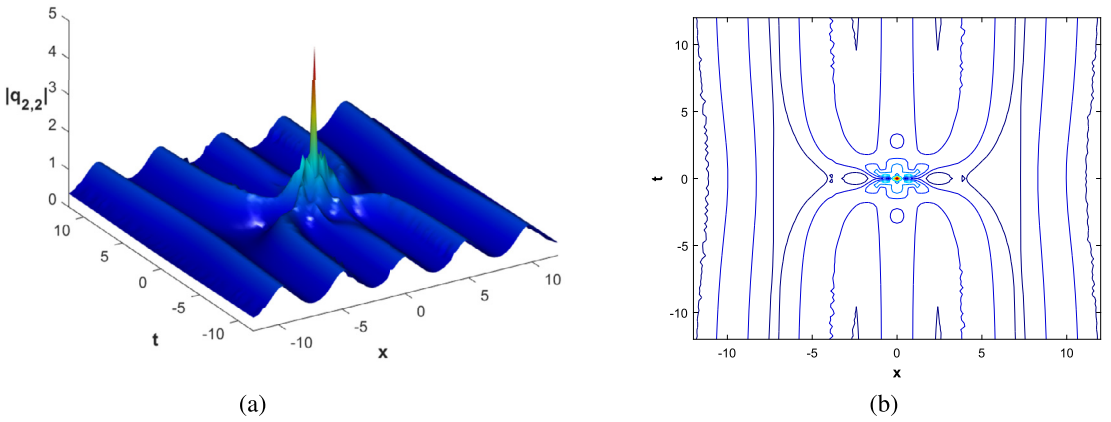

Fig. 7. (a) The second-second-order rogue wave solution on the dn-periodic background with $\alpha = \beta = 1$, $c = 0.675$, $d = 0.325$ and $m = 0.9367$. (b) The contour plot of (a).

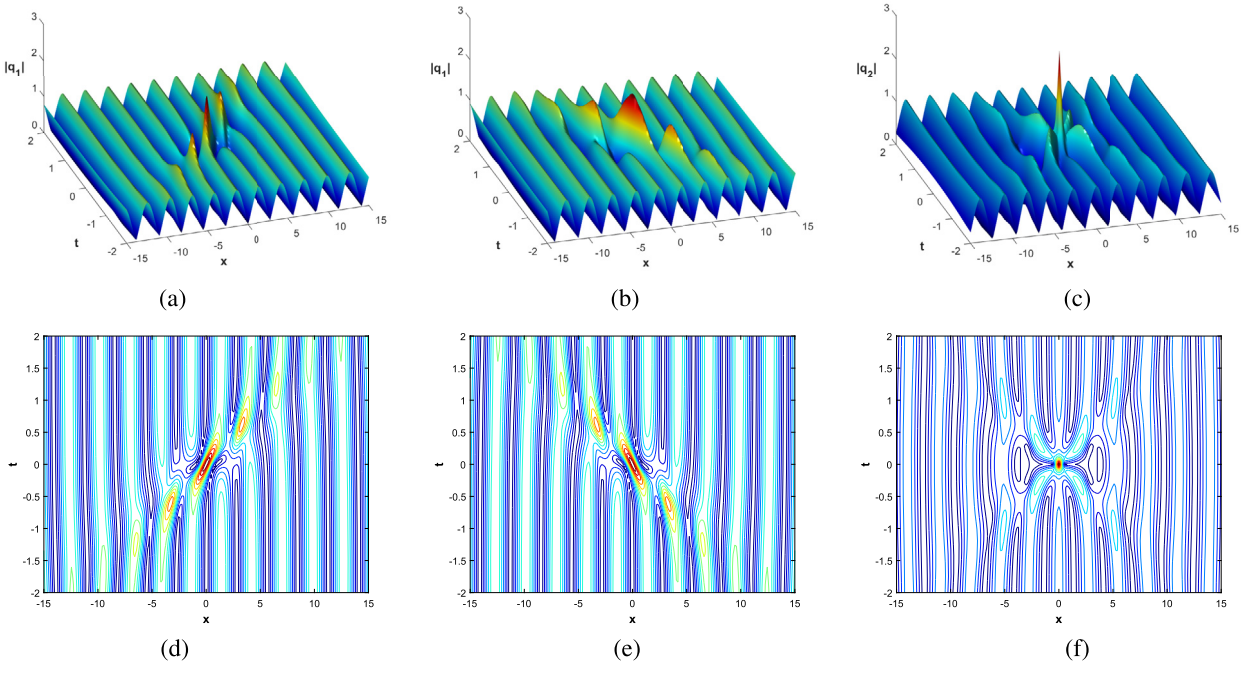

Fig. 8. (a) The first-order cn-rogue wave solution with $\alpha = \beta = 1$, $b = -0.45$, $d = 0.5$ and $m = 0.7433$. (b) The other cn-rogue wave solution with $\alpha = \beta = 1$, $b = 0.45$, $d = 0.5$ and $m = 0.7433$. (c) The second-order cn-rogue wave solution. (d-f) Show the contour plots of the corresponding solutions.

By fixing the amplitude of background: $km = 1$ with the parameters $b = -0.45$ and $d = 0.5$, we plot Fig. 8(a). It shows the spatiotemporal structure of the rogue wave solution on the cn-periodic background with $m = 0.7433$. In this figure, it is obvious that the rogue wave moves to the right, and the maximum value of $|q_1|$ is 2 located at the origin. Moreover, if we take $b = 0.45$ and $d = 0.5$, one can derive another rogue wave moving to the left, which arises from a different branch point, shown in Fig. 8(b). In addition, we can obtain the second-order rogue wave solution by taking $\lambda_1 = -0.45 + 0.5\mathrm{i}$ and $\lambda_2 = 0.45 + 0.5\mathrm{i}$, shown in Fig. 8(c). On the cn-periodic background, a fundamental second-order rogue wave is located at the central part, and its maximum amplitude reaches 3 located at the origin.

Particularly, when $b \to 0$, then $\mathrm{cn}(kx; 1) = \mathrm{sech}(kx)$. Thus, the above rogue wave solutions can also reduce to the double- and third-pole soliton solutions, which agree completely with the results in Section 5.1.

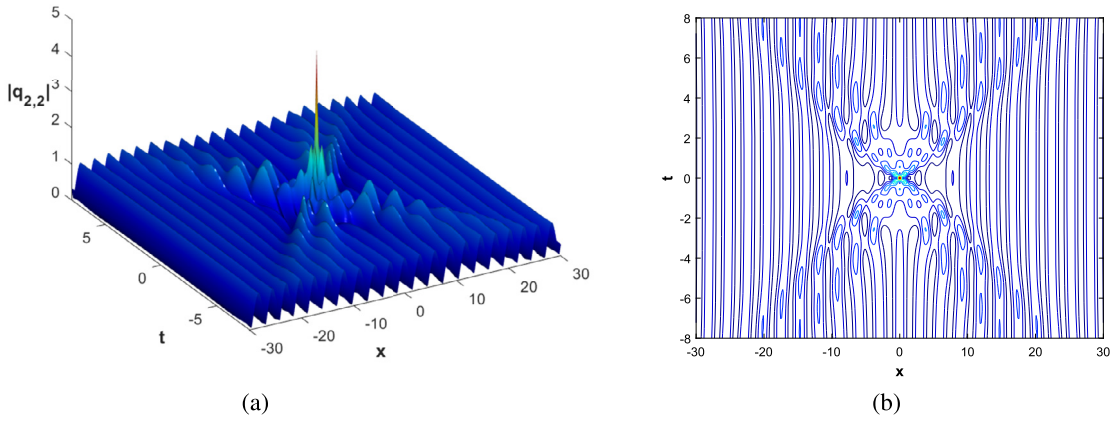

Fig. 9. (a) The second-second-order rogue wave solution on the cn-periodic background with $\alpha = \beta = 1$, $b = 0.2$, $d = 0.5$ and $m = 0.9285$. (b) The contour plot of (a).

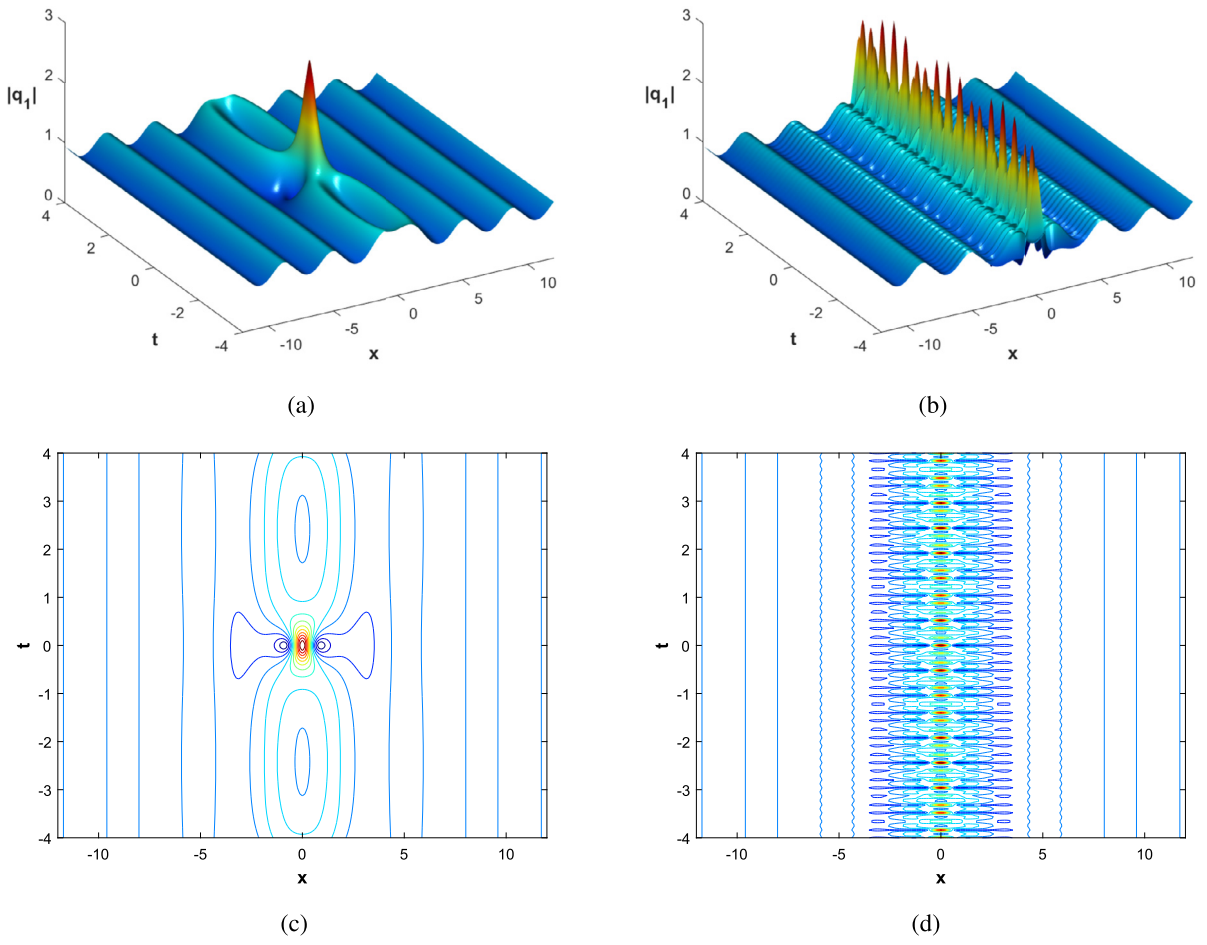

Fig. 10. The KMB on the dn-periodic wave background with the same parameters in Fig. 1(b) except for (a) $\beta = 0.01$ and (b) $\beta = 100$. (c) and (d) respectively show the contour plots of (a) and (b).

By setting $b = 0.2$ and $d = 0.5$, we plot the Fig. 9, which displays the spatiotemporal structures of the second-second-order rogue wave on the cn-periodic background. It seems that four breathers collide and produce a transient high wave at the origin, which corresponds to second-order rogue wave with double poles.

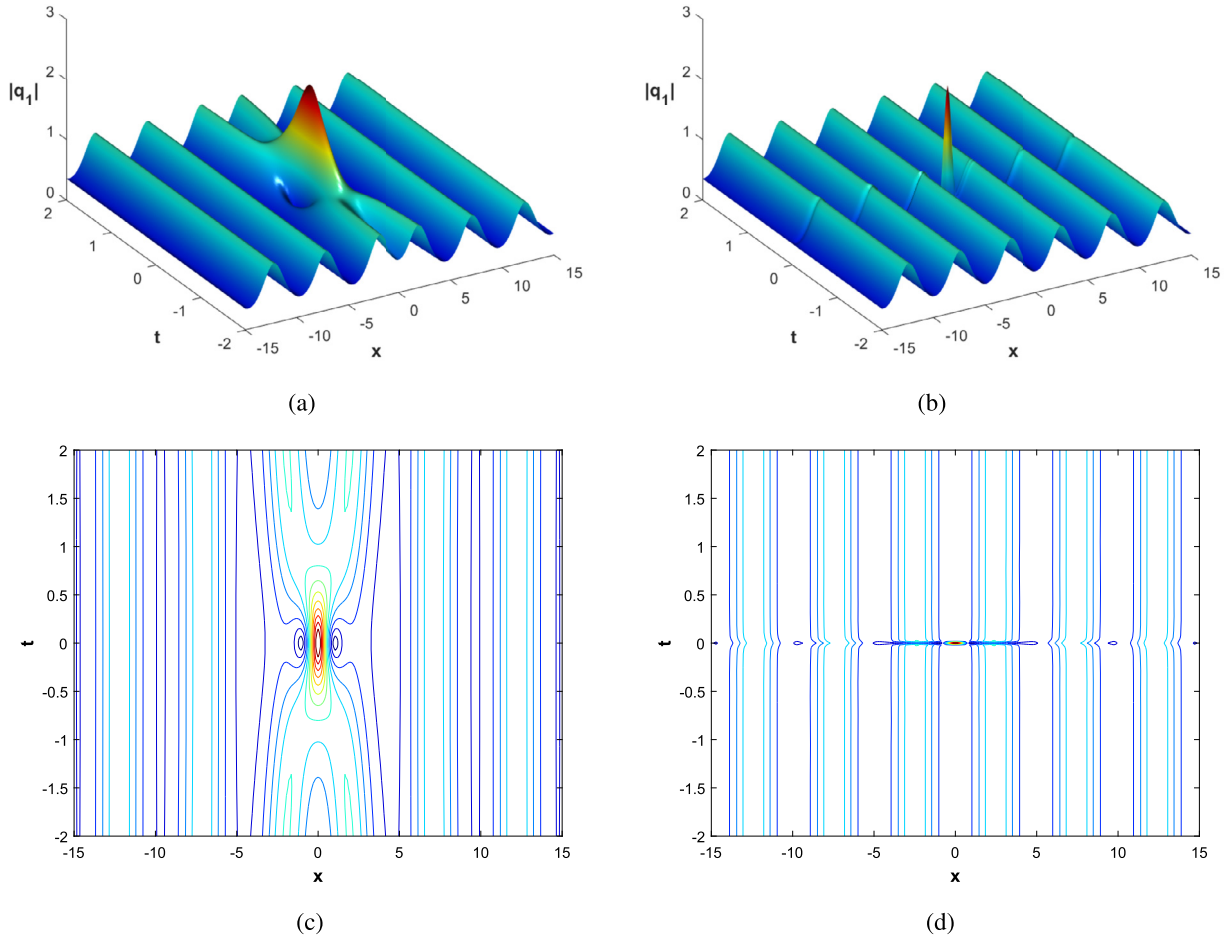

Fig. 11. The rogue wave on the dn-periodic wave background with the same parameters in Fig. 5(a) except for (a) $\beta = 0.01$ and (b) $\beta = 100$. (c) and (d) respectively show the contour plots of (a) and (b).

In addition, the maximum value of the rogue wave can be derived: $|q_{2,2}| = |q(x,t)|+2|2\mathrm{Im}(\lambda_1)|+2|2\mathrm{Im}(\lambda_2)| = 5$.

6. The effects of the parameter β on the breathers and rogue waves

In this section, we mainly discuss how the parameter β (the strength of higher-order nonlinear effects) affects the breathers and rogue waves on the periodic background.

From the expression (62) of the breather on the periodic background, we know that the period of the breathers is $T = 2\pi/\varrho_I$, $\varrho_I = \mathrm{Im}(2\mathrm{i}y(2\alpha + \beta(4s_2 - 8\lambda^2)))$. Therefore, the parameter β can affect the period of the breathers, namely, the period decreases when the value of β increases. Since the parameter β has the similar effect on the GB, KMB and AB on the periodic background, in the following we take the KMB on the dn-periodic wave background as an illustrative example. From three cases in Fig. 10(a), Fig. 1(b) and Fig. 10(b) with $\beta = 0.01$, $\beta = 1$ and $\beta = 100$ respectively, it can be clearly seen that the number of peaks for the breathers on same time interval is increasing when the value of β increases. In addition, the height of peaks of this breather is $|q_1| = q(0,0) + 2|\mathrm{Im}(\lambda(z_1))|$. Therefore, the amplitude and the magnification factor for the breather is independent of the parameter β.

For the purpose of comparison, by choosing three cases of Fig. 11(a), Fig. 5(a) and Fig. 11(b) with the parameter $\beta = 0.01$, $\beta = 1$ and $\beta = 100$ respectively, we show the surface plots of rogue waves on the dn-periodic wave background. It is obvious that the parameter β is responsible for compression effect of

the rogue wave in the time direction. When the value of β increases, the rogue wave compression increases. Similar to the breathers, the parameter β does not affect the amplitude and the magnification factor for the rogue wave on the periodic background.

7. Conclusions

In this paper, we have constructed the multi-breather and higher-order rogue wave solutions of a fourth-order NLS equation on the periodic background. First, by use of the MSW function approach, we have computed a complete family of elliptic solution, which can degenerate into two particular cases, i.e., the dnoidal and cnoidal solutions. In addition, we have solved the corresponding solutions to the associated spectral problem. Second, these solutions have been parameterized via the algebro-geometric method. With the aid of the multifold DT and the additional formulas of the theta functions, we have explicitly expressed the multi-breather solutions in terms of the theta function determinants on the dn and cn periodic backgrounds, which correspond to the parameter $l = \frac{K'}{2}$ and $l = 0$, respectively. On the periodic background, we have constructed three types of multi-breathers: (a) the GB solution; (b) the AB solution; (c) the KMB solution, and two-breather interaction solutions. Moreover, by taking some special limits at the branch points of the breather solutions, we have obtained the first-order, second-order and second-second-order rogue wave solutions on the dn and cn periodic backgrounds. In addition, we have discussed how the parameter β (the strength of higher-order nonlinear effects) affects the breathers and rogue waves on the periodic background.

Data availability

The data that support the findings of this study are available within the article.

Acknowledgments

We express our sincere thanks to the reviewers for their valuable comments. This work is supported by the Natural Science Foundation of Shanghai under Grant No. 18ZR1426600, Science and Technology Commission of Shanghai Municipality.

References

[1] M.J. Ablowitz, J. Satsuma, Solitons and rational solutions of nonlinear evolution equations, J. Math. Phys. 19 (1978) 2180–2186, https://doi.org/10.1063/1.523550.
[2] N. Akhmediev, A. Ankiewicz, J.M. Soto-Crespo, Rogue waves and rational solutions of the nonlinear Schrödinger equation, Phys. Rev. E 80 (2009) 026601, https://doi.org/10.1103/physreve.80.026601.
[3] N. Akhmediev, A. Ankiewicz, M. Taki, Waves that appear from nowhere and disappear without a trace, Phys. Lett. A 373 (2009) 675–678, https://doi.org/10.1016/j.physleta.2008.12.036.
[4] A. Ankiewicz, J.M. Soto-Crespo, N. Akhmediev, Rogue waves and rational solutions of the Hirota equation, Phys. Rev. E 81 (2010) 046602, https://doi.org/10.1103/physreve.81.046602.
[5] A. Ankiewicz, D.J. Kedziora, A. Chowdury, U. Bandelow, N. Akhmediev, Infinite hierarchy of nonlinear Schrödinger equations and their solutions, Phys. Rev. E 93 (2016) 012206, https://doi.org/10.1103/PhysRevE.93.012206.
[6] F. Baronio, M. Conforti, A. Degasperis, S. Lombardo, M. Onorato, S. Wabnitz, Vector rogue waves and baseband modulation instability in the defocusing regime, Phys. Rev. Lett. 113 (2014) 034101, https://doi.org/10.1103/physrevlett.113.034101.
[7] E.D. Belokolos, A.I. Bobenko, V.Z. Enolskii, A.R. Its, V.B. Matveev, Algebro-Geometric Approach to Nonlinear Integrable Equations, Springer, Berlin, 1994.
[8] Y.V. Bludov, V.V. Konotop, N. Akhmediev, Matter rogue waves, Phys. Rev. A 80 (2009) 033610, https://doi.org/10.1103/physreva.80.033610.
[9] P.F. Byrd, M.D. Friedman, Handbook of Elliptic Integrals for Engineers and Scientists, 2nd ed., Springer, Berlin, 1971.
[10] J.B. Chen, D.E. Pelinovsky, Rogue periodic waves of the focusing nonlinear Schrödinger equation, Proc. R. Soc. A 474 (2018) 20170814, https://doi.org/10.1098/rspa.2017.0814.
[11] J.B. Chen, D.E. Pelinovsky, Rogue periodic waves of the modified KdV equation, Nonlinearity 31 (2018) 1955–1980, https://doi.org/10.1088/1361-6544/aaa2da.

[12] J.B. Chen, D.E. Pelinovsky, Rogue waves on the background of periodic standing waves in the derivative nonlinear Schrödinger equation, Phys. Rev. E 103 (2021) 062206, https://doi.org/10.1103/PhysRevE.103.062206.
[13] J.B. Chen, D.E. Pelinovsky, J. Upsal, Modulational instability of periodic standing waves in the derivative NLS equation, J. Nonlinear Sci. 31 (2021) 58, https://doi.org/10.1007/s00332-021-09713-5.
[14] S.H. Chen, F. Baronio, J.M. Soto-Crespo, P. Grelu, D. Mihalache, Versatile rogue waves in scalar, vector, and multidimensional nonlinear systems, J. Phys. A, Math. Theor. 50 (2017) 463001, https://doi.org/10.1088/1751-8121/aa8f00.
[15] S.A. Chin, O.A. Ashour, S.N. Nikolić, M.R. Belić, Peak-height formula for higher-order breathers of the nonlinear Schrödinger equation on nonuniform backgrounds, Phys. Rev. E 95 (2017) 012211, https://doi.org/10.1103/physreve.95.012211.
[16] K.W. Chow, R.H.J. Grimshaw, E. Ding, Interactions of breathers and solitons in the extended Korteweg-de Vries equation, Wave Motion 43 (2005) 158–166, https://doi.org/10.1016/j.wavemoti.2005.09.005.
[17] A. Chowdury, D.J. Kedziora, A. Ankiewicz, N. Akhmediev, Breather solutions of the integrable quintic nonlinear Schrödinger equation and their interactions, Phys. Rev. E 91 (2015) 022919, https://doi.org/10.1103/PhysRevE.91.022919.
[18] A. Chowdury, D.J. Kedziora, A. Ankiewicz, N. Akhmediev, Breather-to-soliton conversions described by the quintic equation of the nonlinear Schrödinger hierarchy, Phys. Rev. E 91 (2015) 032928, https://doi.org/10.1103/physreve.91.032928.
[19] A. Chowdury, W. Krolikowski, N. Akhmediev, Breather solutions of a fourth-order nonlinear Schrödinger equation in the degenerate, soliton, and rogue wave limits, Phys. Rev. E 96 (2017) 042209, https://doi.org/10.1103/physreve.96.042209.
[20] M. Daniel, K. Deepamala, Davydov soliton in alpha helical proteins: higher order and discreteness effects, Physica A 221 (1995) 241–255, https://doi.org/10.1016/0378-4371(95)00243-Z.
[21] M. Daniel, L. Kavitha, R. Amuda, Soliton spin excitations in an anisotropic Heisenberg ferromagnet with octupole-dipole interaction, Phys. Rev. B 59 (1999) 13774–13781, https://doi.org/10.1103/PhysRevB.59.13774.
[22] C.C. Ding, Y.T. Gao, L.Q. Li, Breathers and rogue waves on the periodic background for the Gerdjikov-Ivanov equation for the Alfvén waves in an astrophysical plasma, Chaos Solitons Fractals 120 (2019) 259–265, https://doi.org/10.1016/j.chaos.2019.01.007.
[23] B.F. Feng, L.M. Ling, D.A. Takahashi, Multi-breather and higher-order rogue waves for the nonlinear Schrödinger equation on the elliptic function background, Stud. Appl. Math. 144 (2020) 46–101, https://doi.org/10.1111/sapm.12287.
[24] M. Fleischhauer, A. Imamoglu, J.P. Marangos, Electromagnetically induced transparency: optics in coherent media, Rev. Mod. Phys. 77 (2005) 633–673, https://doi.org/10.1103/revmodphys.77.633.
[25] X.G. Geng, C.W. Cao, Decomposition of the (2+1)-dimensional Gardner equation and its quasi-periodic solutions, Nonlinearity 14 (2001) 1433–1452, https://doi.org/10.1088/0951-7715/14/6/302.
[26] X.G. Geng, Y.T. Wu, Finite-band solutions of the classical Boussinesq-Burgers equations, J. Math. Phys. 40 (1999) 2971–2982, https://doi.org/10.1063/1.532739.
[27] X.G. Geng, J. Shen, B. Xue, A Hermitian symmetric space Fokas-Lenells equation: solitons, breathers, rogue waves, Ann. Phys. 404 (2019) 115–131, https://doi.org/10.1016/j.aop.2019.02.018.
[28] X.G. Geng, R.M. Li, B. Xue, A vector Geng-Li model: new nonlinear phenomena and breathers on periodic background waves, Physica D 434 (2022) 133270, https://doi.org/10.1016/j.physd.2022.133270.
[29] B.L. Guo, L.M. Ling, Q.P. Liu, Nonlinear Schrödinger equation: generalized Darboux transformation and rogue wave solutions, Phys. Rev. E 85 (2012) 026607, https://doi.org/10.1103/physreve.85.026607.
[30] R. Hirota, Exact envelope soliton solutions of a nonlinear wave equation, J. Math. Phys. 14 (1973) 805–809, https://doi.org/10.1063/1.1666399.
[31] A.M. Kamchatnov, On improving the effectiveness of periodic solutions of the NLS and DNLS equations, J. Phys. A 23 (1990) 2945–2960, https://doi.org/10.1088/0305-4470/23/13/031.
[32] A.M. Kamchatnov, New approach to periodic solutions of integrable equations and nonlinear theory of modulational instability, Phys. Rep. 286 (1997) 199–270, https://doi.org/10.1016/S0370-1573(96)00049-X.
[33] A.M. Kamchatnov, Nonlinear Periodic Waves and Their Modulations: An Introductory Course, World Scientific Publishing, Singapore, 2000.
[34] D.J. Kedziora, A. Ankiewicz, N. Akhmediev, Classifying the hierarchy of nonlinear-Schrödinger-equation rogue-wave solutions, Phys. Rev. E 88 (2013) 013207, https://doi.org/10.1103/PhysRevE.88.013207.
[35] D.J. Kedziora, A. Ankiewicz, N. Akhmediev, Rogue waves and solitons on a cnoidal background, Eur. Phys. J. Spec. Top. 223 (2014) 43–62, https://doi.org/10.1140/epjst/e2014-02083-4.
[36] D.J. Kedziora, A. Ankiewicz, A. Chowdury, N. Akhmediev, Integrable equations of the infinite nonlinear Schrödinger equation hierarchy with time variable coefficients, Chaos 25 (2015) 103114, https://doi.org/10.1063/1.4931710.
[37] S. Kharchev, A. Zabrodin, Theta vocabulary I, J. Geom. Phys. 94 (2015) 19–31, https://doi.org/10.1016/j.geomphys.2015.03.010.
[38] C. Kharif, E. Pelinovsky, A. Slunyaev, Rogue Waves in the Ocean, Springer, New York, 2009.
[39] E.A. Kuznetsov, Solitons in a parametrically unstable plasma, Sov. Phys. Dokl. 22 (1977) 507–508.
[40] M. Lakshmanan, K. Porsezian, M. Daniel, Effect of discreteness on the continuum limit of the Heisenberg spin chain, Phys. Lett. A 133 (1988) 483–488, https://doi.org/10.1016/0375-9601(88)90520-8.
[41] M. Li, J.H. Xiao, W.J. Liu, Y. Jiang, K. Sun, B. Tian, Breather and double-pole solutions of the derivative nonlinear Schrödinger equation from optical fibers, Phys. Lett. A 375 (2011) 549–557, https://doi.org/10.1016/j.physleta.2010.12.031.
[42] R.M. Li, X.G. Geng, Rogue periodic waves of the sine-Gordon equation, Appl. Math. Lett. 102 (2019) 106147, https://doi.org/10.1016/j.aml.2019.106147.
[43] R.M. Li, X.G. Geng, Periodic-background solutions for the Yajima-Oikawa long-wave-short-wave equation, Nonlinear Dyn. 109 (2022) 1053–1067, https://doi.org/10.1007/s11071-022-07496-2.
[44] Z.Y. Li, F.F. Li, H.J. Li, Exciting rogue waves, breathers, and solitons in coherent atomic media, Commun. Theor. Phys. 72 (2020) 075003, https://doi.org/10.1088/1572-9494/ab7ed4.

[45] Y.C. Ma, The perturbed plane-wave solutions of the cubic Schrödinger equation, Stud. Appl. Math. 60 (1979) 43–58, https://doi.org/10.1002/sapm197960143.
[46] Y.L. Ma, Interaction and energy transition between the breather and rogue wave for a generalized nonlinear Schrödinger system with two higher-order dispersion operators in optical fibers, Nonlinear Dyn. 97 (2019) 95–105, https://doi.org/10.1007/s11071-019-04956-0.
[47] V.B. Matveev, M.A. Salle, Darboux Transformations and Solitons, Springer, Berlin, 1991.
[48] W.M. Moslem, P.K. Shukla, B. Eliasson, Surface plasma rogue waves, Europhys. Lett. 96 (2011) 25002, https://doi.org/10.1209/0295-5075/96/25002.
[49] S.N. Nikolić, M. Radonjić, N.M. Lučić, A.J. Krmpot, B.M. Jelenković, Transient development of Zeeman electromagnetically induced transparency during propagation of Raman-Ramsey pulses through Rb buffer gas cell, J. Phys. B, At. Mol. Opt. Phys. 48 (2015) 045501, https://doi.org/10.1088/0953-4075/48/4/045501.
[50] S.N. Nikolić, N.B. Aleksić, O.A. Ashour, M.R. Belić, S.A. Chin, Systematic generation of higher-order solitons and breathers of the Hirota equation on different backgrounds, Nonlinear Dyn. 89 (2017) 1637–1649, https://doi.org/10.1007/s11071-017-3540-z.
[51] S.N. Nikolić, O.A. Ashour, N.B. Aleksić, M.R. Belić, S.A. Chin, Breathers, solitons and rogue waves of the quintic nonlinear Schrödinger equation on various backgrounds, Nonlinear Dyn. 95 (2019) 2855–2865, https://doi.org/10.1007/s11071-018-4726-8.
[52] Y. Ohta, J.K. Yang, General high-order rogue waves and their dynamics in the nonlinear Schrödinger equation, Proc. R. Soc. A 468 (2012) 1716–1740, https://doi.org/10.1098/rspa.2011.0640.
[53] D.E. Pelinovsky, R.E. White, Localized structures on librational and rotational travelling waves in the sine-Gordon equation, Proc. R. Soc. A 476 (2020) 20200490, https://doi.org/10.1098/rspa.2020.0490.
[54] W.Q. Peng, S.F. Tian, X.B. Wang, T.T. Zhang, Characteristics of rogue waves on a periodic background for the Hirota equation, Wave Motion 93 (2020) 102454, https://doi.org/10.1016/j.wavemoti.2019.102454.
[55] D.H. Peregrine, Water waves, nonlinear Schrödinger equations and their solutions, J. Aust. Math. Soc. 25 (1983) 16–43, https://doi.org/10.1017/s0334270000003891.
[56] K. Porsezian, V.C. Kuriakose, Optical Solitons: Theoretical and Experimental Challenges, Springer, New York, 2003.
[57] K. Porsezian, M. Daniel, M. Lakshmanan, On the integrability aspects of the one-dimensional classical continuum isotropic biquadratic Heisenberg spin chain, J. Math. Phys. 33 (1992) 1807–1816, https://doi.org/10.1063/1.529658.
[58] K. Porsezian, M. Daniel, M. Lakshmanan, On the integrability aspects of the one-dimensional classical continuum isotropic biquadratic Heisenberg spin chain, J. Math. Phys. 33 (1992) 1807–1816, https://doi.org/10.1063/1.529658.
[59] Z.Y. Qin, G. Mu, Matter, rogue waves in an F = 1 spinor Bose-Einstein condensate, Phys. Rev. E 86 (2012) 036601, https://doi.org/10.1103/physreve.86.036601.
[60] J. Shen, X.G. Geng, B. Xue, Modulation instability and dynamics for the Hermitian symmetric space derivative nonlinear Schrödinger equation, Commun. Nonlinear Sci. Numer. Simul. 78 (2019) 104877, https://doi.org/10.1016/j.cnsns.2019.104877.
[61] A.V. Slunyaev, D.E. Pelinovsky, E.N. Pelinovsky, Rogue waves in the sea: observations, physics, and mathematics, Phys. Usp. 66 (2023) 148–172, https://doi.org/10.3367/UFNe.2021.08.039038.
[62] D.R. Solli, C. Ropers, P. Koonath, B. Jalali, Optical rogue waves, Nature 450 (2007) 1054–1057, https://doi.org/10.1038/nature06402.
[63] D.A. Takahashi, Integrable model for density-modulated quantum condensates: solitons passing through a soliton lattice, Phys. Rev. E 93 (2016) 062224, https://doi.org/10.1103/physreve.93.062224.
[64] L.H. Wang, K. Porsezian, J.S. He, Breather and rogue wave solutions of a generalized nonlinear Schrödinger equation, Phys. Rev. E 87 (2013) 053202, https://doi.org/10.1103/PhysRevE.87.053202.
[65] G. Xu, A. Chabchoub, D.E. Pelinovsky, B. Kibler, Observation of modulation instability and rogue breathers on stationary periodic waves, Phys. Rev. Res. 2 (2020) 033528, https://doi.org/10.1103/physrevresearch.2.033528.
[66] S.W. Xu, J.S. He, L.H. Wang, The Darboux transformation of the derivative nonlinear Schrödinger equation, J. Phys. A 44 (2011) 305203, https://doi.org/10.1088/1751-8113/44/30/305203.
[67] B. Xue, J. Shen, X.G. Geng, Breathers and breather-rogue waves on a periodic background for the derivative nonlinear Schrödinger equation, Phys. Scr. 95 (2020) 055216, https://doi.org/10.1088/1402-4896/ab783e.
[68] Y.Q. Yang, Z.Y. Yan, B.A. Malomed, Rogue waves, rational solitons, and modulational instability in an integrable fifth-order nonlinear Schrödinger equation, Chaos 25 (2015) 103112, https://doi.org/10.1063/1.4931594.
[69] V.E. Zakharov, A.B. Shabat, Exact theory of two-dimensional self-focusing and one-dimensional self-modulation of wave in nonlinear media, Sov. Phys. JETP 34 (1972) 62–69.
[70] V.E. Zakharov, S.V. Manakov, S.P. Novikov, L.P. Pitaevskii, Theory of Solitons, Nauka, Moscow, 1980.
[71] H.Q. Zhang, F. Chen, Rogue waves for the fourth-order nonlinear Schrödinger equation on the periodic background, Chaos 31 (2021) 023129, https://doi.org/10.1063/5.0030072.
[72] H.Q. Zhang, X. Gao, Z.J. Pei, F. Chen, Rogue periodic waves in the fifth-order Ito equation, Appl. Math. Lett. 107 (2020) 106464, https://doi.org/10.1016/j.aml.2020.106464.
[73] J.H. Zhang, L. Wang, C. Liu, Superregular breathers, characteristics of nonlinear stage of modulation instability induced by higher-order effects, Proc. R. Soc. A 473 (2017) 20160681, https://doi.org/10.1098/rspa.2016.0681.